Bioorganic & Medicinal Chemistry 17 (2009) 5549–5564

Contents lists available at ScienceDirect

Bioorganic & Medicinal Chemistry

journal homepage: www.elsevier.com/locate/bmc

Synthesis, cannabinoid receptor affinity, molecular modeling studies and in vivo pharmacological evaluation of new substituted 1-aryl-5-(1*H*-pyrrol-1-yl)-1*H*-pyrazole-3-carboxamides. 2. Effect of the 3-carboxamide substituent on the affinity and selectivity profile

Romano Silvestri [a,*], Alessia Ligresti [b], Giuseppe La Regina [a], Francesco Piscitelli [a,†], Valerio Gatti [a], Antonella Brizzi [c], Serena Pasquini [c], Antonio Lavecchia [d,*], Marco Allarà [b], Noemi Fantini [e], Mauro Antonio Maria Carai [e], Ettore Novellino [d], Giancarlo Colombo [e], Vincenzo Di Marzo [b], Federico Corelli [c,*]

[a] *Istituto Pasteur—Fondazione Cenci Bolognetti, Dipartimento di Studi Farmaceutici, Sapienza Università di Roma, Piazzale Aldo Moro 5, I-00185 Roma, Italy*
[b] *Istituto di Chimica Biomolecolare, Consiglio Nazionale delle Ricerche, Via Campi Flegrei 34, Comprensorio Olivetti, I-80078 Pozzuoli, Napoli, Italy*
[c] *Dipartimento Farmaco Chimico Tecnologico, Università di Siena, Polo Scientifico Universitario San Miniato, Via Aldo Moro 2, I-53100 Siena, Italy*
[d] *Dipartimento di Chimica Farmaceutica e Tossicologica, Università di Napoli Federico II, Via Domenico Montesano 49, I-80131 Napoli, Italy*
[e] *Istituto di Neuroscienze, Consiglio Nazionale delle Ricerche, Viale Diaz 182, I-09126 Cagliari, Italy*

ARTICLE INFO

Article history:
Received 8 April 2009
Revised 9 June 2009
Accepted 14 June 2009
Available online 21 June 2009

Keywords:
Cannabinoid
Human recombinant CB receptor type 1
Pyrrole bioisoteres
Structure–activity relationships
Molecular modeling

ABSTRACT

New substituted 1-aryl-5-(1*H*-pyrrol-1-yl)-1*H*-pyrazole-3-carboxamides were synthesized by replacing the 2,4-dichlorobenzyl and cyclohexyl moieties at the 3-carboxamide nitrogen of the previously reported CB_1 receptor antagonists/inverse agonists **4** and **5**. Several ligands showed potent affinity for the hCB_1 receptor, with K_i concentrations comparable to the reference compounds **1**, **4** and **5**, and exhibited CB_1 selectivity comparable to **1** and **2**. Docking experiments and molecular dynamics (MD) simulations explained the potent hCB_1 binding affinity of compounds **31** and **37**. According to our previous studies, **31** and **37** formed a H-bond with K3.28(192), which accounted for the high affinity for the receptor inactive state and the inverse agonist activity. The finding of inhibition of food intake following their acute administration to rats, supported the concept that the CB_1 selective compounds **4** and **52** act as antagonists/inverse agonists.

1. Introduction

Cannabinoid CB_1 and CB_2 receptors have become intriguing targets for the development of new drugs, because of their involvement in an ever growing number of pathological conditions, such as pain, immunosuppression, peripheral vascular disease, appetite enhancement or suppression, and locomotor disorders.[1] Rimonabant (SR141716, **1**) is a potent and selective CB_1 receptor inverse agonist which was launched in 2006 by Sanofi-Aventis for the treatment of overweight and obesity, and some associated cardiovascular and metabolic disorders.[2] In clinical trials, the major adverse effects associated with **1** were gastrointestinal; however, depression and anxiety also became apparent at the daily dose of 20 mg.[3] In 2008, Sanofi-aventis suspended the marketing of **1** by acknowledging EMEA's recommendation.[4]

New CB ligands have been actively searched either by synthesis of pyrazole analogues of **1** (such as the CB_1 selective AM251 (**2**) and CB_2 selective SR144528 (**3**) ligands) (Chart 1), or replacement of the central pyrazole nucleus with a bioisosteric heterocyclic ring.[5a] More recently, new CB ligands have been developed by following a non-bioisosteric approach.[5b] Our studies on pyrrole bioisosteric analogues[6] prompted the design of new CB ligands by replacing the 4-chlorophenyl group at position 5 of **1** with a pyrrole nucleus.[7] Compound **4**, bearing a 2,4-dichlorophenyl group at position 1 and a 2,5-dimethylpyrrole moiety at position 5 of the pyrazole ring, was highly selective for the human recombinant CB_1 receptor and showed a CB_1 selectivity index (SI) calculated as $K_i(CB_2)/K_i(CB_1)$ ratio of 140. On the other hand, compound **5** (K_i = 5.6 nM) was equipotent to **2** as a hCB_1 ligand. Both compounds behaved as inverse agonists in the cAMP assay.[7]

* Corresponding authors. Tel.: +39 06 4991 3800; fax: +39 06 491 491 (R.S.); tel./fax: +39 081 678 613 (A.L.); tel.: +39 0577 234308; fax: +39 0577 234299 (F.C.).
E-mail addresses: romano.silvestri@uniroma1.it (R. Silvestri), lavecchi@unina.it (A. Lavecchia), corelli@unisi.it (F. Corelli).
† Present address: University of Pennsylvania, Department of Chemistry, 231 South 34th Street, Philadelphia, PA 19104-6323, USA.

0968-0896/$ - see front matter © 2009 Elsevier Ltd. All rights reserved.
doi:10.1016/j.bmc.2009.06.027

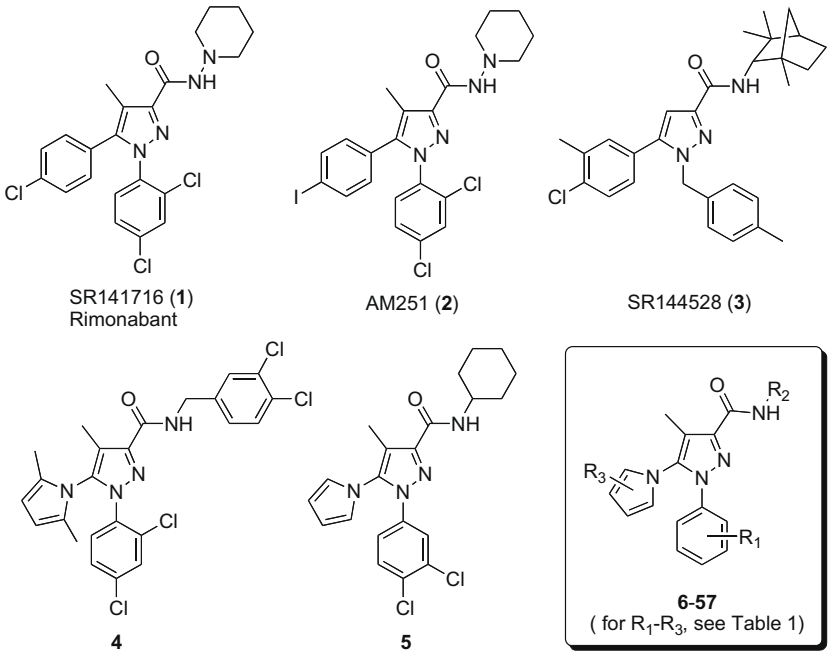

Chart 1. Reference and new CB ligands.

The substituent groups at the 3-carboxamide were not exhaustively explored. We modified here the 2,4-dichlorobenzyl at the 3-carboxamide nitrogen of **4**, by changing both number and position of the substituents at the phenyl ring, and length of the alkyl spacer. The cyclohexyl group of **5** was replaced by cyclohomologues and some correlated cycloalkyl substituents (compounds **6–57**, Table 1). The methyl groups at the positions 2 and 5 of the pyrrole ring were either maintained or removed, while the 2,4- and 3,4-dihalophenyl rings at the position 1 of the pyrazole were not modified.

Docking experiments and molecular dynamics (MD) simulations were carried out using a previously developed model of the hCB_1 receptor in its inactive form.[7] The most active compounds were docked into this receptor model and the observed ligand–receptor interactions were discussed, also taking into account the site-directed mutagenesis data available for this receptor subtype.

2. Results

2.1. Chemistry

Carboxamides **6–57** were obtained through parallel synthesis in 62–98% yield by coupling reaction of acids **58–63**, in turn prepared as previously described,[7] with selected amines in the presence of *N*-(3-dimethylaminopropyl)-*N*′-ethylcarbodiimide hydrochloride (EDC) and 1-hydroxybenzotriazole (HOBt), using morpholinomethyl-polystyrene and polymer bound *p*-toluensulfonic acid as scavengers for acidic and basic substances, respectively (Scheme 1 and Table 1).

2.2. Biology

The binding affinities (K_i values) of compounds **6–57** for human recombinant CB_1 (hCB_1) and CB_2 (hCB_2) receptors, evaluated in parallel with CB_1 (**1** and **2**) and CB_2 (**3**) reference compounds, are shown in Table 1. The previously described pyrazoles **4** and **5**[7] are included for comparison purpose. The CB_1 and CB_2 receptor binding of tested compounds was evaluated by means of membranes from HEK cells transfected with either the hCB_1 or hCB_2 receptor and [^{3}H]-(−)-*cis*-3-[2-hydroxy-4-(1,1-dimethylheptyl)-phenyl]-*trans*-4-(3-hydroxypropyl)cyclohexanol ([^{3}H]-CP-55,940). As described by the manufacturer (Perkin–Elmer, Italy), the high affinity ligand K_d values were 0.18 nM for CB_1 receptor, and 0.31 nM for CB_2 receptor.[8] Incubating the drugs with [^{3}H]CP-55,940 at 0.14 nM for CB_1 and 0.084 nM for CB_2 binding assay, allowed to derive the displacement curves. K_i values were calculated by applying the Cheng–Prusoff equation[9] to the IC_{50} values (from GraphPad) for the displacement of the bound radioligand at increasing concentrations of tested compound.

Administration of compound **1**, as well as other cannabinoid CB_1 receptor antagonists/inverse agonists, dose-dependently suppresses food intake and reduces body weight in lean and obese rats and mice.[10,11] Here, we evaluated the effect of the acute administration of the highly CB_1 selective compounds **4** and **52** on food intake in rats given unlimited access to regular food pellets and water.

2.3. Discussion

The new 5-(1*H*-pyrrol-1-yl)pyrazole-3-carboxamides elicited remarkable affinity and/or selectivity characteristics. Several carboxamides (**18**, **23**, **27**, **29**, **30**, **35, 36**, **50**, **52–55**, and **57**) were high affinity ligands for the hCB_1 receptor, and showed K_i values in the same range of concentrations of the reference compounds **1** and **4**. Carboxamides **28**, **31**, and **37** showed the highest affinities for the hCB_1 receptor with K_i values at low nanomolar concentration, and were equipotent to **2** and **5**. CB_1 SIs (calculated as $K_i(CB_2)/K_i(CB_1)$ ratios) of derivatives **9**, **15**, **16**, **18**, **43**, **50**, **52**, and **53** were superior the reference compounds **1** and **2**. Compounds **28**, **30**, **31**, **36**, and **38** showed hCB_2 receptor binding affinities comparable to the CB_2 reference compound **3** and the previously reported pyrazole **5**.[7] Moreover, **38** and **30** possess also significant CB_2 selectivity, **38** being the most CB_2-selective compound identified in this study.

The affinity for the hCB_1 receptor was affected by both nature and position of the substituents on the phenyl ring at position 1 of the pyrazole nucleus. Generally speaking, the chloro derivatives

Table 1
Structure, hCB1 and hCB2 receptor affinity (K_i values, nM) of new derivatives **6**–**57**, reference compounds **1**–**3**, and previously described derivatives **4**, **5**[a]

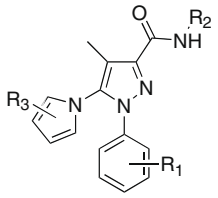

4-57

Compound	R_1	R_2	R_3	K_i[b,c] (nM)		
				hCB1[d,f]	hCB2[e,f]	SI[g]
6	2,4-Cl_2	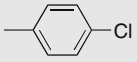	H	120	80	0.67
7	2,4-Cl_2	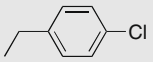	H	140	940	6.71
8	2,4-Cl_2	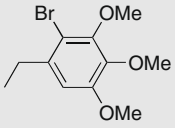	H	227	609	2.68
9	2,4-Cl_2	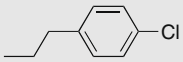	H	70	>3940	>56.2
10	2,4-Cl_2	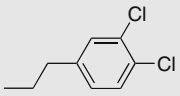	H	157	>3940	>25.09
11	2,4-Cl_2	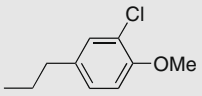	H	368	2887	7.84
12	2,4-Cl_2	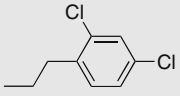	H	218	>3940	>18.07
13	2,4-Cl_2		H	84	170	2.02
14	2,4-Cl_2	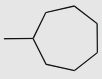	H	20	20	1.00
15	2,4-Cl_2	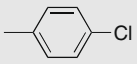	2,5-Me_2	96	>3940	>41.04
16	2,4-Cl_2		2,5-Me_2	90	>3940	>43.78
17	2,4-Cl_2	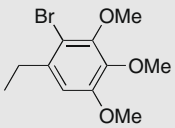	2,5-Me_2	144	553	3.84
18	2,4-Cl_2	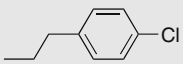	2,5-Me_2	30	>3940	>131.33
19	2,4-Cl_2	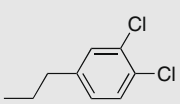	2,5-Me_2	117	>3940	33.36
20	2,4-Cl_2	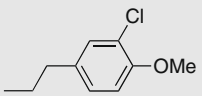	2,5-Me_2	112	3483	31.09

(*continued on next page*)

Table 1 (*continued*)

Compound	R_1	R_2	R_3	K_i[b,c] (nM)		
				hCB1[d,f]	hCB2[e,f]	SI[g]
21	2,4-Cl_2	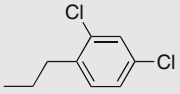	2,5-Me_2	156	>3940	>25.25
22	2,4-Cl_2		2,5-Me_2	150	310	2.07
23	2,4-Cl_2	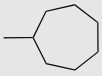	2,5-Me_2	56	80	1.43
24	3,4-Cl_2	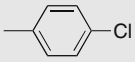	H	1300	790	0.61
25	3,4-Cl_2	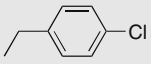	H	70	100	1.43
26	3,4-Cl_2	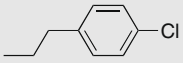	H	240	1200	5.0
27	3,4-Cl_2		H	50	12	0.24
28	3,4-Cl_2	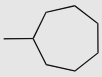	H	5.6	1.3	0.23
29	3,4-Cl_2	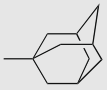	H	31	20	0.65
30	3,4-Cl_2	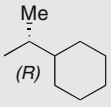	H	14	1.6	0.11
31	3,4-Cl_2	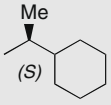	H	3.4	2.4	0.71
32	3,4-Cl_2	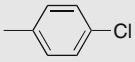	2,5-Me_2	>2820	>3940	–
33	3,4-Cl_2	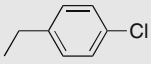	2,5-Me_2	100	790	7.90
34	3,4-Cl_2	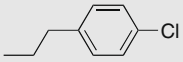	2,5-Me_2	390	>3940	>10.10
35	3,4-Cl_2		2,5-Me_2	36	12	0.33
36	3,4-Cl_2	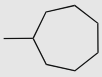	2,5-Me_2	12	4.2	0.35
37	3,4-Cl_2	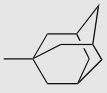	2,5-Me_2	5.6	12	2.14
38	3,4-Cl_2	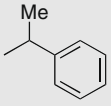	2,5-Me_2	80	5.7	0.071

Table 1 (*continued*)

Compound	R_1	R_2	R_3	K_i[b,c] (nM)		
				hCB1[d,f]	hCB2[e,f]	SI[g]
39	3,4-Cl_2	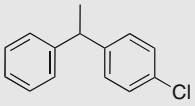	2,5-Me_2	>2820	>3940	—
40	2,4-F_2	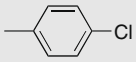	H	2100	>3940	3.76
41	2,4-F_2	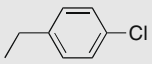	H	340	3400	10.0
42	2,4-F_2	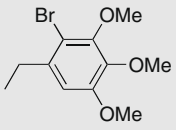	H	345	739	2.14
43	2,4-F_2	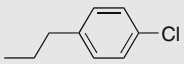	H	80	>3940	>49.25
44	2,4-F_2	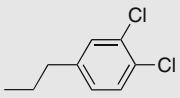	H	310	1291	4.16
45	2,4-F_2	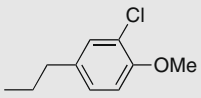	H	948	1945	2.05
46	2,4-F_2	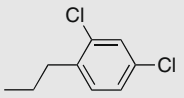	H	380	667	1.75
47	2,4-F_2		H	2400	1100	0.46
48	2,4-F_2	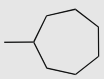	H	560	200	0.36
49	2,4-F_2	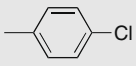	2,5-Me_2	560	>3940	>7.04
50	2,4-F_2	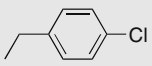	2,5-Me_2	56	>3940	>70.36
51	2,4-F_2	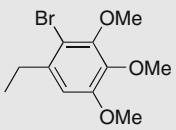	2,5-Me_2	165	373	2.26
52	2,4-F_2	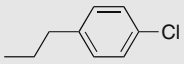	2,5-Me_2	50	>3940	>78.80
53	2,4-F_2	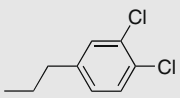	2,5-Me_2	54	>3940	>72.96
54	2,4-F_2	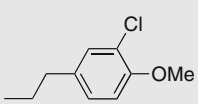	2,5-Me_2	99	>3940	>39.79
55	2,4-F_2	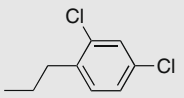	2,5-Me_2	41	721	17.58

(*continued on next page*)

Table 1 (*continued*)

Compound	R_1	R_2	R_3	K_i[b,c] (nM)		
				hCB1[d,f]	hCB2[e,f]	SI[g]
56	2,4-F_2		2,5-Me_2	840	900	1.07
57	2,4-F_2	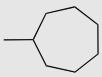	2,5-Me_2	56	110	1.96
1[h]	—	—	—	12	790	65.83
2[i]	—	—	—	2.3	112	48.70
3[j]	—	—	—	>2820	5.4	<0.002
4[k,l]	2,4-Cl_2	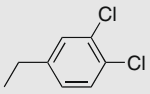	2,5-Me_2	28	3940	140.7
5[k,l]	3,4-Cl_2		H	5.6	1.7	0.30

[a] Data represent mean values for at least three separate experiments performed in duplicate and are expressed as K_i (nM). Standard error of means (SEM) are not shown for the sake of clarity and were never higher than 5% of the means.
[b] K_i: equilibrium dissociation constant, that is the concentration of the competing ligand that will bind to half the binding sites at equilibrium, in the absence of radioligand or other competitors.
[c] IC_{50}: The concentration of competitor that competes for half of the specific binding. This is the measure of the competitor's potency at interacting with the receptor against the radioligand.
[d] hCB_1: human CB_1 receptor.
[e] hCB_2: human CB_2 receptor.
[f] For both receptor binding assays, the new compounds were tested using membranes from HEK cells transfected with either the hCB_1 or hCB_2 receptor and [^{3}H]-(−)-*cis*-3-[2-hydroxy-4-(1,1-dimethylheptyl)-phenyl]-*trans*-4-(3-hydroxy-propyl)-cyclohexanol ([^{3}H]CP-55,940).
[g] SI: CB_1 selectivity index was calculated as $K_i(CB_2)/K_i(CB_1)$ ratio.
[h] Compound **1**: Rimonabant, CB_1 reference compound.
[i] Compound **2**: AM251, CB_1 reference compound.
[j] Compound **3**: SR144528, CB_2 reference compound.
[k] The binding affinities of reference compounds **1**–**3** were evaluated in parallel with compounds **6**–**57** under the same conditions.
[l] Lit.[7]

were more potent than their fluorinated counterparts (for an example, compare **14** and **28** with **48,** and **6** with **40**). The 2,4-dichlorophenyl substituent allowed the ligands to be more selective for the CB_1 receptor than the corresponding 3,4-dichlorophenyl analogs (compare **9** with **26**, **15** with **32, 16** with **33,** and **18** with **34**) (Chart 2).

On the other hand, hCB_1 receptor affinity was greatly affected by the substitution pattern of the pyrrole nucleus at position 5. Derivatives bearing both the 5-(2,5-dimethylpyrrole) and 1-(2,4-dihalophenyl) groups showed generally greater affinity for the hCB_1 receptor than the corresponding compounds deprived of the methyl groups. This trend tends to reverse in the 3,4-dichlorophenyl series. Most importantly, the 2,5-dimethylpyrroles were more selective for the hCB_1 receptor in both the 1-(2,4-dichlorophenyl) and 1-(2,4-difluorophenyl) series (compare **6** with **15**, **7** with **16**, and **46** with **53**).

Affinity and selectivity for the hCB_1 receptor were also affected by the substituent at the 3-carboxamide group. A 4-chloro- or 3,4-dichlorophenyl ring linked at the nitrogen of the carboxamide provided ligands endowed with high selectivity (although not with the strongest affinity) for the hCB_1 receptor (compounds **4**, **9**, **15**, **16**, **18**, **43**, **50**, **52**, and **53**). Such an effect was mostly due to the lack of affinity of these derivatives for the hCB_2 receptor. The presence of methoxy groups resulted in a decrease of both affinity and selectivity (compare **4** with **17**, **18** with **20**, and **53** with **54**).

The spacer group between the phenyl ring and the nitrogen of the carboxamide also played a crucial role. With the only exception of **15**, derivatives lacking this spacer showed weak affinity (**24**, **32**,

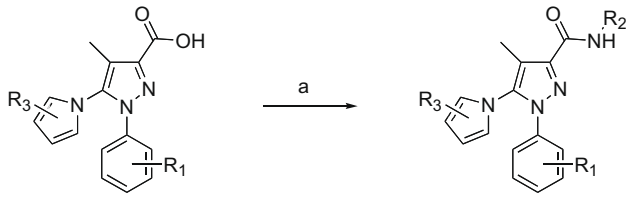

58-63 **6-57**

58: R_1 = 2,4-Cl_2; R_3 = H; **59**: R_1 = 2,4-Cl_2; R_3 = 2,5-Me_2; **60**: R_1 = 3,4-Cl_2; R_3 = H; **61**: R_1 = 3,4-Cl_2; R_3 = 2,5-Me_2; **62**: R_1 = 2,4-F_2; R_3 = H; **63**: R_1 = 2,4-F_2; R_3 = 2,5-Me_2.
6-57: for R_1-R_3 substituents, see Table 1.

Scheme 1. Synthesis of derivatives **6-57.** Reagents and reaction conditions. (a) (i) R_2NH_2, HOBt, EDC, dichloromethane, 0 °C to rt, overnight; (ii) morpholinomethyl-polystyrene and polymer bound *p*-toluensulfonic acid, rt, 24 h.

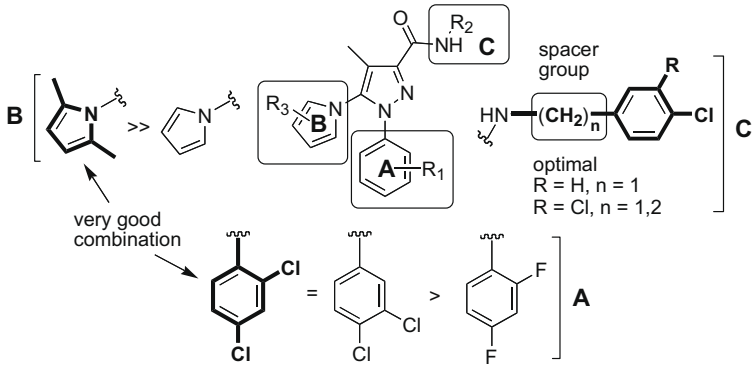

Chart 2. SAR summary for high hCB_1 receptor affinity and selectivity.

40, **49**) or low selectivity (**6**) for the hCB_1 receptor, while the introduction of a methylene spacer resulted in an increase of hCB_1 receptor selectivity. Further extension of the spacer substantially retained the selectivity for the hCB_1 receptor (**9**, **18**, **43**, **52** and **53**).

Because of the potent affinity displayed by **5**[7] for both CB_1 and CB_2 receptors, we synthesized new derivatives bearing a cyclopentyl, cyclohexyl or cycloheptyl group at the 3-carboxamide. Among them, derivatives **28** and **36**, exhibiting a 1-(3,4-dichlorophenyl) ring, showed strong affinity for both receptor subtypes.

As above-mentioned, the high selectivity of derivatives **4**, **9**, **15**, **16**, **18**, **43**, **50**, **52** and **53** for the hCB_1 receptor was basically due to the lack of affinity for the CB_2 subtype. The presence of a $(CH_2)_nAr$ (where $n = 0–2$) system at the 3-carboxamide nitrogen proved to be detrimental for the hCB_2 receptor affinity. In an attempt to improve the CB_2 selectivity, new compounds bearing 1-adamantyl, 1-cyclohexylethyl or 1-phenylethyl groups as substituents at the carboxamide nitrogen were synthesized. Although derivatives **30**, **31**, **37** and **38** still exhibited high affinity for both receptors, **38** is presently the second most CB_2-selective ligand in our hands. Moreover, a certain degree of enantioselectivity was also highlighted, with the (*R*)-enantiomer **30** showing approximately sixfold higher selectivity for the hCB_2 receptor than the corresponding (*S*)-isomer **31**. This result suggests that a substituent at C1 of the spacer group might play a positive role for either affinity or selectivity for both receptor subtypes.

2.4. Molecular modeling

The binding mode of **1** into hCB_1 receptor was extensively investigated through SAR, mutagenesis, and molecular modeling studies.[7,12–17] Key features were: (i) an aromatic cluster formed by F3.25(190), F3.36(200), W4.64(255), W5.43(279), W6.48(356), and Y5.39(275) that is in contact with the two phenyl rings of **1** through aromatic stacking interactions;[14] (ii) K3.28(192) that forms a H-bond with the amide carbonyl oxygen of **1**. It was proposed, this interaction may stabilize the putative inactive state of hCB_1 receptor.[13,15] S7.39(383), which resides across from K3.28(192) in the active site, appears to have no direct interaction with **1**.[12] To explain the potent hCB_1 binding affinity of compounds **31** and **37**, we built a docking model of both hCB_1/**31** and hCB_1/**37** complexes using our previously published homology model of the inactive state of hCB_1.[7] Initial structures of the hCB_1 complexes were generated by means of the automatic docking program GOLD, version 4.0,[18] defining the bound **1** in the hCB_1 bundle[7] as a reference. In this pose, the carboxamide oxygens of both ligands were H-bonded to K3.28(192), while the 3,4-dichlorophenyl rings at position 1 of the pyrazole were close to F3.36(200), Y5.39(275), and W5.43(279) residues, in well agreement with previous combined mutation/modeling studies.[14,15]

To assess the stability of the complexes, we performed 1 ns MD simulations at a constant temperature of 300 K. During the MD simulations, the rmsd of the protein compared to the starting hCB_1 model structure was quite stable (<1 Å rmsd, data not shown). The rmsd of the ligands remained low (<2 Å, data not shown) and did not vary significantly between the two compounds. The average rmsd variation of the heavy atoms of selected amino acid residues within a 15 Å radius from the drug molecule was 0.98 ± 0.1 Å. Such a result indicates that both orientation and conformation of the amino acids involved in ligand binding were also well preserved.

Figures 1 and 2 clearly show that the carboxamide oxygens of **31** and **37** were able to form H-bond with K3.28(192) (this particular interaction was present for the whole simulation time). Such H-bond interaction accounted for the high affinity of **1** for the inactive receptor state and its inverse agonism activity.[15] According to our previous modeling studies,[7] a H-bond between the carbonyl oxygen of **1** and the K3.28(192) residue stabilizes a salt bridge between K3.28(192) and D6.58(366). Formation of this H-bond increases the affinity and shifts the receptor equilibrium toward the inactive state.[16,19]

The two docking models displayed: (i) the 3,4-dichlorophenyl ring at position 1 of the pyrazole system resided in a hydrophobic pocket formed by L3.29(193), F3.36(200), I4.56(247), W5.43(279), M6.55(363), V6.59(367), and established favorable π–π stacking interactions with the indole ring of W5.43(279) and the phenyl ring of F3.36(200). Such interactions, which involve the aromatic residue-rich TM3-4-5-6 region of hCB_1[14] (colored magenta in Figs. 1 and 2), were very stable during the MD trajectory (the electron-withdrawing chlorine substituents contribute to strength the π-stacking interactions); (ii) the 5-pyrrole ring of **31** resided in a pocket formed by F3.36(200), W6.48(356) and L6.51(359). In contrast, the 2,5-dimethylpyrrole ring of **37** formed contacts with the hydrophobic residue V3.32(196), and projected the two methyl groups close to the lipophilic residues L7.43(387) and L3.29(193); (iii) the 4-methyl group of **31** formed hydrophobic interactions with I6.54(362) and L6.51(359) residues, while that of **37** interacted with L7.43(387); (iv) Ser7.39(383), although located near the amide bond, did not form any H-bond with both ligands; (v) the N-substituents of the carboxamide were embedded within a lipophilic pocket made up by the side chains of Q1.31(116), I1.34(119), F2.57(170), F2.61(174), F2.64(177), F7.35(379), A7.36(380), C7.42(386) and L7.43(387). Worthy to note, this lipophilic pocket can accommodate aromatic groups bearing electron-withdrawing substituents (as reported in our previous paper,[7] the 3,4-dichlorobenzyl ring of **4** maintained direct aromatic stacking interactions with both F2.61(174) and F2.64(177).

Accordingly, the electron-withdrawing chlorine atoms decrease the electron density at the aromatic ring, thereby improving the

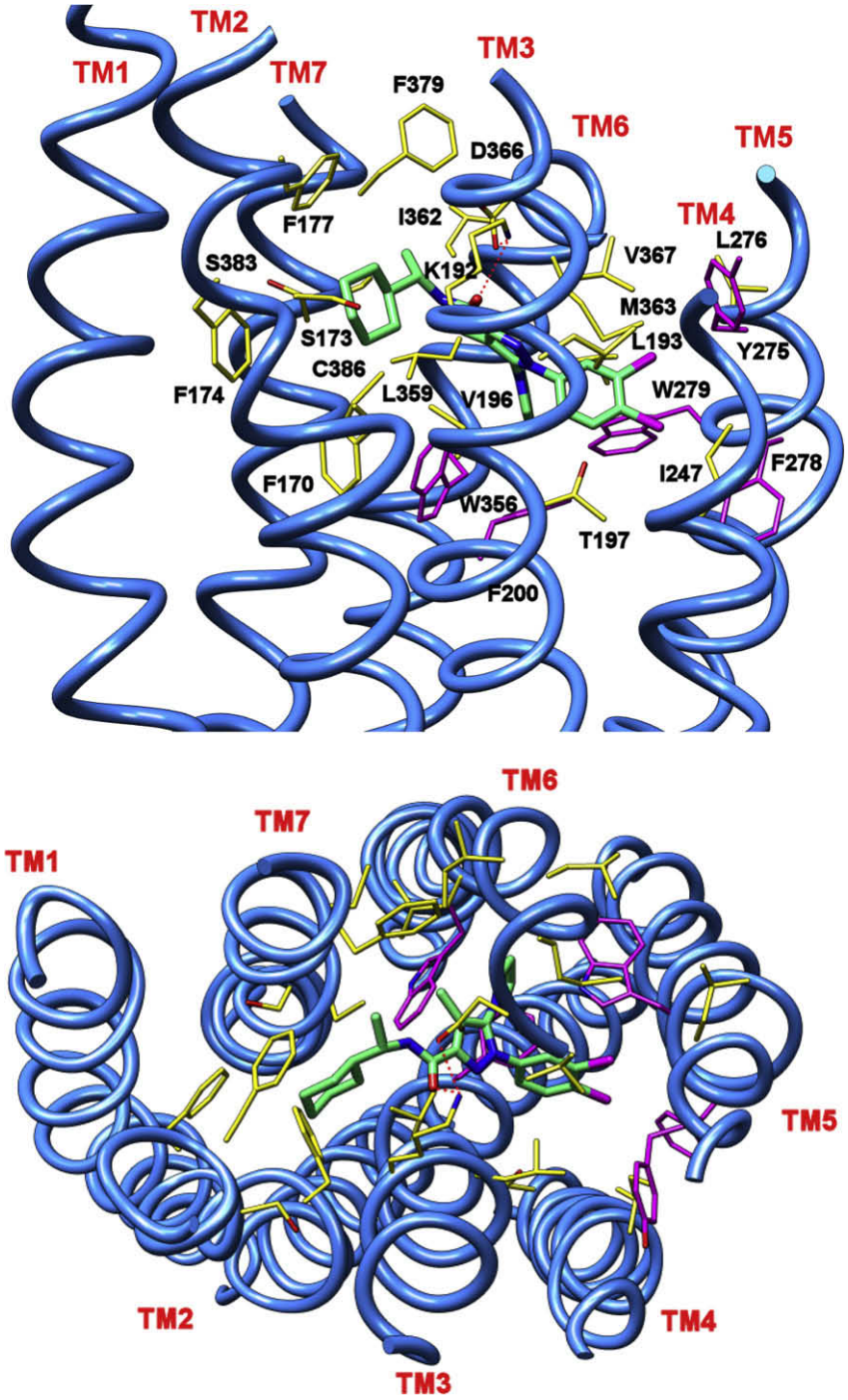

Figure 1. Complex of the hCB_1 receptor with compound **31**. View from the plane of the cell membrane of the **31**/hCB_1 complex (top view). View from outside the cell of the **31**/hCB_1complex (bottom view). Only amino acids located within 4 Å distance from the ligand (green–blue) are shown in yellow and labeled. Residues that form part of the aromatic cluster complex with ligand are colored in magenta. H-bonds are indicated by dashed red lines.

affinity of the ligands for the hCB_1 receptor; on the contrary, the electron-donating methoxy groups increase the electron density at the aromatic ring, thereby decreasing the affinity of the ligands for the hCB_1 receptor. Such findings are consistent with the activity trend showed by our series of compounds (compare **4** with **17**, **18** with **20**, and **53** with **54**); (vi) consistently with a nice accommodation of the (*S*)-α-methyl group into a small cavity delimited by the aromatic residues F2.64(177) and F7.35(379), carboxamide **31** showed (moderately) greater hCB_1 binding affinity than the corresponding (*R*)-**30** (**31**, K_i = 3.4 nM; **30**, K_i = 14 nM). The binding models of **31** and **37** generated by docking analysis and MD simulations provided new insight for the design of potent and selective hCB_1 ligands.

2.5. In vivo pharmacological studies

ANOVA revealed a significant effect of acute treatment with compound **4** on cumulative food intake over the first 360 min after lights off [$F(3,28) = 15.89$, $P < 0.0001$]. *Post hoc* analysis revealed that 1 and 10 mg/kg of compound **4** significantly reduced cumulative food intake, with respect to vehicle, at each time interval (Fig. 3, top panel). Percent reduction in cumulative food intake in

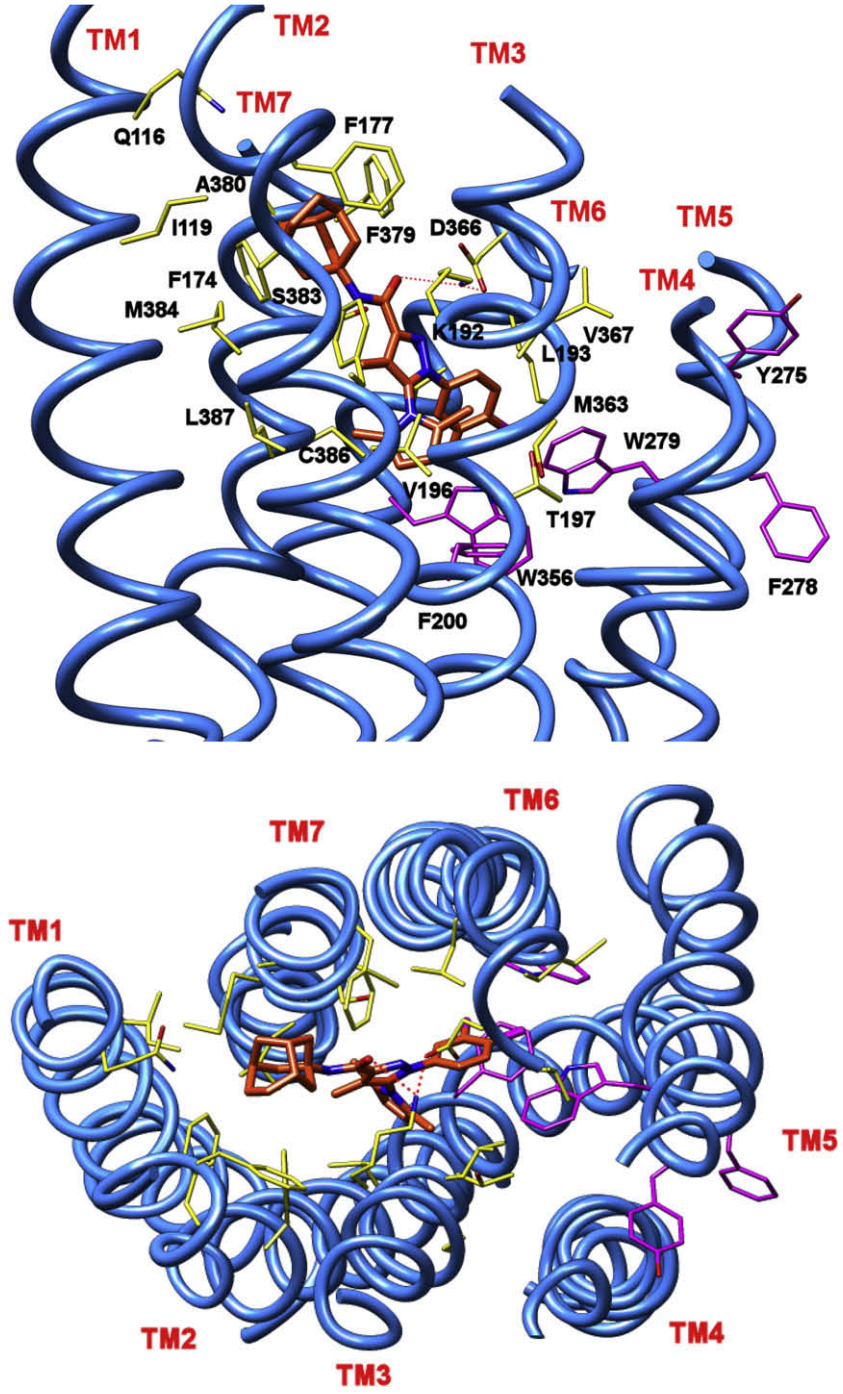

Figure 2. Complex of the hCB_1 receptor with compound **37**. View from the plane of the cell membrane of the **37**/hCB_1 complex (top view). View from outside the cell of the **37**/hCB_1complex (bottom view). Only amino acids located within 4 Å distance from the ligand (green–blue) are shown in yellow and labeled. Residues that form part of the aromatic cluster complex with ligand are colored in magenta. H-bonds are indicated by dashed red lines.

the rat groups treated with 1 and 10 mg/kg of compound **4** ranged between 15 and 30 and between 25 and 40, respectively. At the 1440-min time interval, a tendency toward a reduction in food intake in the rat groups treated with 1 and 10 mg/kg of compound **4** was still observed [$F(3,28) = 2.74$, $P = 0.061$] (Fig. 3, top panel). The reducing effect of compound **4** was specific for food intake, as treatment with this compound did not affect cumulative water intake over the first 360 min after lights off [$F(3,28) = 0.95$, $P > 0.05$] and water intake at the 1440-min time interval [$F(3,28) = 1.57$, $P > 0.05$] (Fig. 3, bottom panel).

ANOVA revealed a significant effect of acute treatment with compound **52** on cumulative food intake over the first 360 min after lights off [$F(3,23) = 3.20$, $P < 0.05$]. *Post hoc* analysis revealed that 1 mg/kg of compound **52** significantly reduced cumulative food intake, with respect to vehicle, only at the 360-min time interval (Fig. 4, top panel).

Conversely, 10 mg/kg of compound **52** significantly reduced cumulative food intake, with respect to vehicle, at each time interval (Fig. 4, top panel). Percent reduction in cumulative food intake in the rat group treated with 10 mg/kg of compound **52** ranged between 25 and 45. At the 1440-min time interval, a tendency toward a reduction in food intake in the rat group treated with 10 mg/kg of compound **52** was still observed [$F(3,23) = 2.46$, $P = 0.088$] (Figure ure4, top panel).

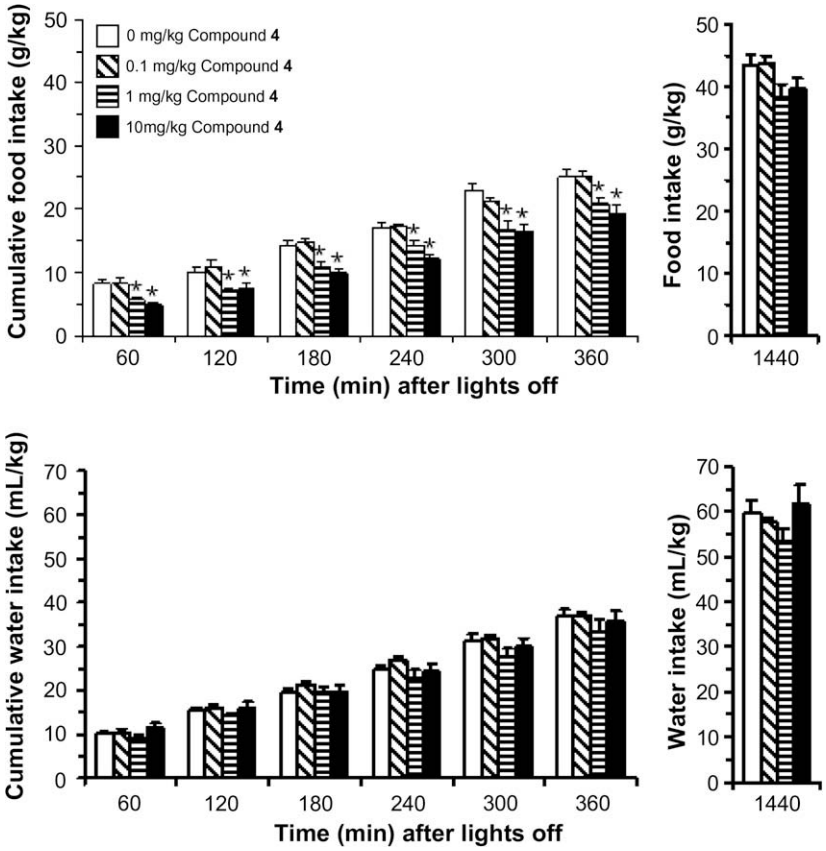

Figure 3. Effect of the acute administration of different doses of compound **4** on food (top panel) and water (bottom panel) intake in Wistar rats given unlimited access to regular rodent chow and water. Each bar is the mean ± S.E.M. of $n = 8$ rats. *:P <0.05 with respect to vehicle-treated rats at the same time interval (Newman–Keuls test).

The inhibitory effect of compound **52** was specific for food intake, as treatment with this compound did not affect cumulative water intake over the first 360 min after lights off [$F(3,23) = 1.90$, $P > 0.05$] and water intake at the 1440-min time interval [$F(3,23) = 1.60$, $P > 0.05$] (Fig. 4, bottom panel).

These results indicate that doses of compounds **4** and **52** included between 1 and 10 mg/kg may reduce food intake in non-obese rats. Compound **4** appeared to be more potent than compound **52**, as 1 mg/kg of compound **4** was able to significantly reduce cumulative food intake at each time interval between 60 and 360 min; vice versa, 1 mg/kg of compound **52** significantly reduced cumulative food intake only at the 360-min time interval. Conversely, both drugs displayed comparable efficacy, with their highest dose (10 mg/kg) exerting a similar effect (40–45% reduction in comparison to vehicle-treated rats at the 60-min time interval). Compounds **4** and **52** had also a comparable duration of effect: at the 1440-min time interval, both drugs produced only a tendency towards a reduction of food intake.

3. Conclusions

Several ligands showed potent affinity for the hCB_1 receptor, with K_i concentrations comparable to the reference compounds **1**, **4** and **5**, and exhibited CB_1 selectivity comparable to **1** and **2**. The chloro derivatives were more potent ligands than their fluorinated counterparts. Both 5-(2,5-dimethylpyrrole) and 1-(2,4-dihalophenyl) groups led to great affinity for the hCB_1 receptor. The 1-(2,4-dichlorophenyl)pyrazoles were more CB_1 selective than the corresponding 3,4-dichlorophenyl analogs. Introduction of a methylene spacer resulted in an increase of hCB_1 receptor selectivity. Docking experiments and molecular dynamics (MD) simulations showed that carboxamide oxygens of **31** and **37** formed H-bond with K3.28(192), as for **1**.[7] Acute administration of compounds **4** and **52** in rats led to appetite suppression and anorectic effect. Such findings in an in vivo pharmacological set up confirm that **4** and **52** act as antagonists/inverse agonists at CB_1 receptors. Although we have not fully reached the goal to obtain both potent and selective CB_1 ligands, these findings represent a useful basis for the design of new analogues.

4. Experimental

4.1. Chemistry

4.1.1. Materials and methods

Melting points (mp) were determined on a Büchi 510 apparatus and are uncorrected. Infrared spectra (IR) were run on Perkin–Elmer 1310 and SpectrumOne spectrophotometers. Band position and absorption ranges are given in cm^{-1}. Proton nuclear magnetic resonance (^1H NMR) spectra were recorded on Bruker AM-200 (200 MHz) and Bruker Avance 400 MHz FT spectrometers in the indicated solvent. Chemical shifts are expressed in δ units (ppm) from tetramethylsilane. Column chromatographies were packed with alumina (Merck, 70–230 mesh) and silica gel (Merck, 70–230 mesh). Aluminum oxide TLC cards (Fluka, aluminum oxide precoated aluminum cards with fluorescent indicator at 254 nm) and silica gel TLC cards (Fluka, silica gel precoated aluminum cards with fluorescent indicator at 254 nm) were used for thinlayer chromatography (TLC). Developed plates were visualized with a Spectroline ENF 260C/F UV apparatus. Organic solutions were dried over anhydrous sodium sulfate. Evaporation of the solvents was carried out on a Büchi Rotavapor R-210 equipped with a Büchi V-850 vacuum controller and Büchi V-700 (~5 mbar) and V-710 vacuum (~2 mbar) pumps. Elemental analyses were found within ±0.4%

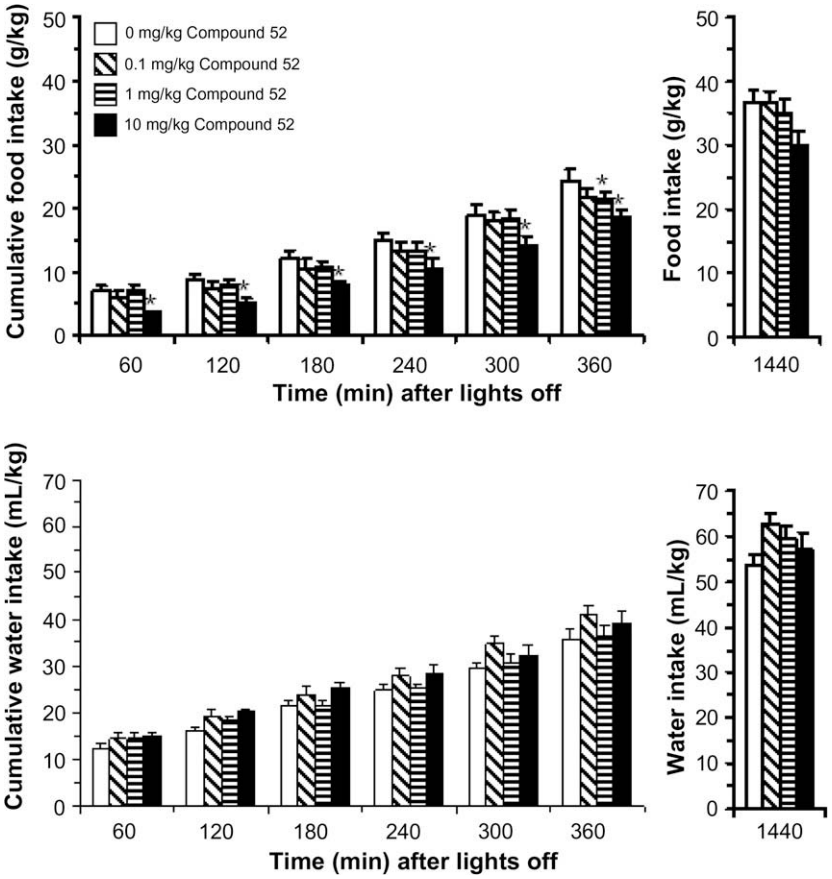

Figure 4. Effect of the acute administration of different doses of compound **52** on food (top panel) and water (bottom panel) intake in Wistar rats given unlimited access to regular rodent chow and water. Each bar is the mean ± S.E.M. of $n = 6–7$ rats. *: $P < 0.05$ with respect to vehicle-treated rats at the same time interval (Newman–Keuls test).

of the theoretical values. Purity of tested compounds was >95%. Büchi Syncore reactor was used for parallel synthesis, filtration, and evaporation.

4.1.2. Parallel synthesis of amides 6–57

To a solution of an appropriate acid **58–63** (1 mmol) in dichloromethane, kept at 0 °C, *N*-(3-dimethylaminopropyl)-*N*′-ethylcarbodiimide (EDC, 1.2 mmol) and 1-hydroxybenzotriazole (HOBt, 1.0 mmol) were added followed by the appropriate amine (1.5 mmol). The solutions were allowed to warm up to room temperature and placed in the Büchi Syncore reactor. The reactions were stirred at 300 rpm overnight and then morpholinomethylpolystyrene (3 equiv/mol) was added. After 1 h at room temperature, polymer bound *p*-toluensulfonic acid (3 equiv/mol) was added and the mixtures were stirred at room temperature for additional 24 h. The mixtures were filtered and the resulting solutions were evaporated to dryness under reduced pressure. Purification of the crude products by crystallization from dichloromethane (unless otherwise stated) gave carboxamides **6–57**.

4.1.2.1. *N*-(4-Chlorophenyl) 1-(2,4-dichlorophenyl)-4-methyl-5-(1*H*-pyrrol-1-yl)-1*H*-pyrazole-3-carboxamide (6). Yield 83% as a white solid, mp 180 °C. ^{1}H NMR ($CDCl_3$): δ 2.33 (s, 3H), 6.19–6.21 (m, 2H), 6.58–6.59 (m, 2H), 7.19–7.24 (m, 1H), 7.28 (d, 2H, $J = 8.3$ Hz), 7.47 (d, 1H, $J = 1.6$ Hz), 7.61 (d, 2H, $J = 8.8$ Hz), 8.75 (s, 1H). IR: ν 1689 cm^{-1}. MS *m/z*: 467 [M+23]$^+$ (100).

4.1.2.2. *N*-(4-Chlorobenzyl) 1-(2,4-dichlorophenyl)-4-methyl-5-(1*H*-pyrrol-1-yl)-1*H*-pyrazole-3-carboxamide (7). Yield 90% as white solid, mp 135 °C. ^{1}H NMR ($CDCl_3$): δ 2.30 (s, 3H), 4.55 (d, 2H, $J = 6.8$ Hz), 6.18–6.19 (m, 2H), 6.56–6.57 (m, 2H), 7.11–7.33 (m, 6H), 7.39–7.44 (m, 1H). IR: ν 1673 cm^{-1}. MS *m/z*: 460 [M+1]$^+$, 482 [M+23]$^+$ (100).

4.1.2.3. *N*-(2-Bromo-3,4,5-trimethoxybenzyl) 1-(2,4-dichlorophenyl)-4-methyl-5-(1*H*-pyrrol-1-yl)-1*H*-pyrazole-3-carboxamide (8). Yield 95% as a pale yellow oil. ^{1}H NMR ($CDCl_3$): δ 2.29 (s, 3H), 3.83 (s, 3H), 3.85 (s, 3H), 3.87 (s, 3H), 4.64 (d, 2H, $J = 6.4$ Hz), 6.18–6.19 (m, 2H), 6.54–6.56 (m, 2H), 6.87 (s, 1H), 7.19–7.28 (m, 2H), 7.38 (br t, 1H, $J = 6.0$ Hz), 7.44 (d, 1H, $J = 2.3$ Hz). IR: ν 1672 cm^{-1}. MS *m/z*: 595 [M+1]$^+$ (100), 617 [M+23]$^+$.

4.1.2.4. *N*-[2-(4-Chlorophenyl)ethyl] 1-(2,4-dichlorophenyl)-4-methyl-5-(1*H*-pyrrol-1-yl)-1*H*-pyrazole-3-carboxamide (9). Yield 98% as a colorless oil. ^{1}H NMR ($CDCl_3$): δ 2.29 (s, 3H), 2.86 (t, 2H, $J = 7.1$ Hz), 3.56–3.67 (m, 2H), 6.17–6.19 (m, 2H), 6.55–6.56 (m, 2H), 7.03 (br t, 1H, $J = 5.7$ Hz), 7.12–7.25 (m, 6H), 7.43–7.44 (m, 1H). IR: ν 1671 cm^{-1}. MS *m/z*: 474 [M+1]$^+$ (100), 496 [M+23]$^+$, 969 [2M+23]$^+$.

4.1.2.5. *N*-[2-(3,4-Dichlorophenyl)ethyl] 1-(2,4-dichlorophenyl)-4-methyl-5-(1*H*-pyrrol-1-yl)-1*H*-pyrazole-3-carboxamide (10). Yield 95% as a colorless oil. ^{1}H NMR ($CDCl_3$): δ 2.28 (s, 3H), 2.86 (t, 2H, $J = 7.0$ Hz), 3.57–3.67 (m, 2H), 6.17–6.19 (m, 2H), 6.55–6.56 (m, 2H), 7.01 (br t, 1H, $J = 5.7$ Hz), 7.05 (dd, 1H, $J = 1.9$ Hz, $J = 8.5$ Hz), 7.14–7.34 (m, 4H), 7.44 (d, 1H, $J = 1.9$ Hz). IR: ν 1672 cm^{-1}. MS *m/z*: 509 [M+1]$^+$, 531 [M+23]$^+$ (100).

4.1.2.6. *N*-[2-(3-Chloro-4-methoxyphenyl)ethyl] 1-(2,4-dichlorophenyl)-4-methyl-5-(1*H*-pyrrol-1-yl)-1*H*-pyrazole-3-carboxamide (11). Yield 75% as a white solid, mp 140 °C. ^{1}H NMR ($CDCl_3$): δ 2.28 (s, 3H), 2.82 (t, 2H, $J = 7.1$ Hz), 3.55–3.66 (m, 2H), 3.85 (s, 3H),

6.18–6.19 (m, 2H), 6.54–6.55 (m, 2H), 6.84 (d, 2H, J = 8.5 Hz), 7.09–7.28 (m, 3H), 7.44 (d, 1H, J = 1.8 Hz). IR: ν 1670 cm^{-1}. MS m/z: 504 $[M+1]^+$, 526 $[M+23]^+$ (100).

4.1.2.7. *N*-[2-(2,4-Dichlorophenyl)ethyl] 1-(2,4-dichlorophenyl)-4-methyl-5-(1*H*-pyrrol-1-yl)-1*H*-pyrazole-3-carboxamide (12). Yield 90% as a white oil. ^1H NMR ($CDCl_3$): δ 2.29 (s, 3H), 3.02 (t, 2H, J = 7.1 Hz), 3.60–3.70 (m, 2H), 6.18–6.19 (m, 2H), 6.55–6.56 (m, 2H), 7.14–7.27 (m, 4H), 7.36 (s, 1H), 7.45 (d, 2H, J = 2.0 Hz). IR: ν 1666 cm^{-1}. MS m/z: 509 $[M+1]^+$, 531 $[M+23]^+$ (100).

4.1.2.8. *N*-Cyclopentyl 1-(2,4-dichlorophenyl)-4-methyl-5-(1*H*-pyrrol-1-yl)-1*H*-pyrazole-3-carboxamide (13). Yield 98% as a white solid, mp 63 °C (from diethyl ether). ^1H NMR ($CDCl_3$): δ 1.32–1.43 (m, 2H), 1.47–1.59 (m, 2H), 1.63–1.71 (m, 2H), 1.97–2.09 (m, 2H), 2.28 (s, 3H), 4.27–4.44 (m, 1H), 6.15–6.17 (m, 2H), 6.53–6.55 (m, 2H), 6.85 (br d, 1H, J = 7.4 Hz), 7.17–7.28 (m, 2H), 7.43 (d, 1H, J = 1.8 Hz). IR: ν 1662 cm^{-1}. MS m/z: 403 $[M+1]^+$, 425 $[M+23]^+$ (100), 829 $[2M+23]^+$.

4.1.2.9. *N*-Cycloheptyl 1-(2,4-dichlorophenyl)-4-methyl-5-(1*H*-pyrrol-1-yl)-1*H*-pyrazole-3-carboxamide (14). Yield 95% as white needles, mp 178 °C (from diethyl ether). ^1H NMR ($CDCl_3$): δ 1.51–1.65 (mm, 8H), 1.96–2.06 (m, 4H), 2.27 (s, 3H), 4.03–4.19 (m, 1H), 6.16–6.18 (m, 2H), 6.54–6.55 (m, 2H), 6.86 (br d, 1H), 717–7.28 (m, 2H), 7.43 (d, 1H, J = 1.6 Hz). IR: ν 1663 cm^{-1}. MS m/z: 431 $[M+1]^+$, 453 $[M+23]^+$ (100).

4.1.2.10. *N*-(4-Chlorophenyl) 1-(2,4-dichlorophenyl)-5-(2,5-dimethyl-1*H*-pyrrol-1-yl)-4-methyl-1*H*-pyrazole-3-carboxamide (15). Yield 77% as a pale yellow pasty solid. ^1H NMR ($CDCl_3$): δ 1.96 (s, 6H), 2.22 (s, 3H), 5.81 (s, 2H), 6.91 (d, 1H, J = 8.7 Hz), 7.20 (dd, 1H, J = 2.0 Hz, J = 8.6 Hz), 7.30 (d, 2H, J = 8.6 Hz), 7.52 (d, 1H, J = 2.0 Hz), 7.64 (d, 2H, J = 8.8 Hz), 8.69 (s, 1H). IR: ν 1687 cm^{-1}. MS m/z: 473 $[M+1]^+$, 495 $[M+23]^+$ (100).

4.1.2.11. *N*-(4-Chlorobenzyl) 1-(2,4-dichlorophenyl)-5-(2,5-dimethyl-1*H*-pyrrol-1-yl)-4-methyl-1*H*-pyrazole-3-carboxamide (16). Yield 91% as a white solid, mp 153.6 °C. ^1H NMR ($CDCl_3$): δ 1.94 (s, 6H), 2.19 (s, 3H), 4.58 (d, 2H, J = 6.3 Hz), 5.80 (s, 2H), 6.87 (d, 2H, J = 8.7 Hz), 7.16 (dd, 1H, J = 1.8 Hz, J = 8.8 Hz), 7.22–7.35 (m, 3H), 7.38 (br t, 1H, 6.0 Hz), 7.47 (d, 1H, J = 2.3 Hz),. IR: ν 1672 cm^{-1}. MS m/z: 488 $[M+1]^+$, 510 $[M+23]^+$ (100).

4.1.2.12. *N*-(2-Bromo-3,4,5-trimethoxybenzyl) 1-(2,4-dichlorophenyl)-5-(2,5-dimethyl-1*H*-pyrrol-1-yl)-4-methyl-1*H*-pyrazole-3-carboxamide (17). Yield 97% as a white solid, mp 186–187 °C. ^1H NMR ($CDCl_3$): δ 1.92 (s, 6H), 2.17 (s, 3H), 3.85 (s, 6H), 3.87 (s, 3H), 4.65 (d, 2H, J = 6.1 Hz), 5.78 (s, 2H), 6.88 (s, 1H), 7.13–7.19 (m, 2H), 7.49 (d, 1H, J = 1.9 Hz). IR: ν 1671 cm^{-1}. MS m/z: 623 $[M+1]^+$ (100), 645 $[M+23]^+$.

4.1.2.13. *N*-[2-(4-Chlorophenyl)ethyl] 1-(2,4-dichlorophenyl)-5-(2,5-dimethyl-1*H*-pyrrol-1-yl)-4-methyl-1*H*-pyrazole-3-carboxamide (18). Yield 98% as a cream solid, mp 139.6 °C. ^1H NMR ($CDCl_3$): δ 1.93 (s, 6H), 2.18 (s, 3H), 2.89 (t, 2H, J = 7.1 Hz), 3.59–3.69 (m, 2H), 5.79 (s, 2H), 6.84 (d, 2H, J = 8.7 Hz), 7.07 (br t, 1H, J = 6.3 Hz), 7.13–7.27 (m, 4H), 7.50 (d, 1H, J = 2.2 Hz). IR: ν 1666 cm^{-1}. MS m/z: 503 $[M+1]^+$, 525 $[M+23]^+$.

4.1.2.14. *N*-[2-(3,4-Dichlorophenyl)ethyl] 1-(2,4-dichlorophenyl)-5-(2,5-dimethyl-1*H*-pyrrol-1-yl)-4-methyl-1*H*-pyrazole-3-carboxamide (19). Yield 95% as a yellow solid, mp 121 °C. ^1H NMR ($CDCl_3$): δ 1.93 (s, 6H), 2.17 (s, 3H), 2.88 (t, 2H, J = 7.0 Hz), 3.59–3.69 (m, 2H), 5.79 (s, 2H), 6.85 (d, 2H, J = 8.8 Hz), 7.07 (dd, 1H, J = 1.7 Hz, J = 7.8 Hz), 7.16 (dd, 1H, J = 1.9 Hz, J = 8.8 Hz), 7.34 (d, 1H, J = 8.3 Hz), 7.49 (d, 1H, J = 2.0 Hz). IR: ν 1671 cm^{-1}. MS m/z: 537 $[M+1]^+$, 559 $[M+23]^+$ (100).

4.1.2.15. *N*-[2-(3-Chloro-4-methoxyphenyl)ethyl] 1-(2,4-dichlorophenyl)-5-(2,5-dimethyl-1*H*-pyrrol-1-yl)-4-methyl-1*H*-pyrazole-3-carboxamide (20). Yield 90% as a yellow oil. ^1H NMR ($CDCl_3$): δ 1.93 (s, 6H), 2.17 (s, 3H), 2.84 (t, 2H, J = 7.1 Hz), 3.57–3.68 (m, 2H), 3.86 (s, 3H), 5.79 (s, 2H), 6.85 (d, 2H, J = 8.3 Hz), 7.04 (br t, 1H, J = 5.2 Hz), 7.07–7.19 (m, 3H), 7.49 (d, 1H, J = 2.0 Hz). IR: ν 1666 cm^{-1}. MS m/z: 532 $[M+1]^+$, 554 $[M+23]^+$ (100).

4.1.2.16. *N*-[2-(2,4-Dichlorophenyl)ethyl] 1-(2,4-dichlorophenyl)-5-(2,5-dimethyl-1*H*-pyrrol-1-yl)-4-methyl-1*H*-pyrazole-3-carboxamide (21). Yield 94% as a white solid, mp 135 °C. ^1H NMR ($CDCl_3$): δ 1.93 (s, 6H), 2.17 (s, 3H), 3.03 (t, 2H, J = 7.3 Hz), 3.61–3.72 (m, 2H), 5.79 (s, 2H), 7.06 (br t, 1H, J = 5.7 Hz), 7.14–7.37 (m, 3H), 7.50 (d, 1H, J = 2.7 Hz). IR: ν 1659 cm^{-1}. MS m/z: 537 $[M+1]^+$, 559 $[M+23]^+$ (100).

4.1.2.17. *N*-Cyclopentyl 1-(2,4-dichlorophenyl)-5-(2,5-dimethyl-1*H*-pyrrol-1-yl)-4-methyl-1*H*-pyrazole-3-carboxamide (22). Yield 84% as colorless needles, mp 121 °C. ^1H NMR ($CDCl_3$): δ 1.43–1.71 (mm, 6H), 1.92(s, 6H), 1.98–2.10 (m, 2H), 2.16 (s, 3H), 4.32–4.42 (m, 1H), 5.77 (s, 2H), 6.93 (d, 1H, J = 8.5 Hz), 7.16 (dd, 1H, J = 1.9 Hz, J = 8.5 Hz), 7.48 (d, 1H, J = 2.1 Hz). IR: ν 1661 cm^{-1}. MS m/z: 431 $[M+1]^+$, 453 $[M+23]^+$ (100), 883 $[2M+23]^+$.

4.1.2.18. *N*-Cycloheptyl 1-(2,4-dichlorophenyl)-5-(2,5-dimethyl-1*H*-pyrrol-1-yl)-4-methyl-1*H*-pyrazole-3-carboxamide (23). Yield 85% as a pale yellow solid, mp 128 °C. ^1H NMR ($CDCl_3$): δ 1.51–1.76 (mm, 8H), 1.92 (s, 6H), 1.97–2.07 (m, 4H), 2.16 (s, 3H), 4.03–4.17 (m, 1H), 5.78 (s, 2H), 6.88 (d, 1H, J = 8.8 Hz), 6.94 (br s, 1H), 7.15 (dd, 1H, J = 2.1 Hz, J = 8.9 Hz), 7.48 (s, 1H). IR: ν 1660 cm^{-1}. MS m/z: 459 $[M+1]^+$, 481 $[M+23]^+$ (100).

4.1.2.19. *N*-(4-Chlorophenyl) 1-(3,4-dichlorophenyl)-4-methyl-5-(1*H*-pyrrol-1-yl)-1*H*-pyrazole-3-carboxamide (24). Yield 96% as white needles, mp 196 °C (from diethyl ether). ^1H NMR ($CDCl_3$): δ 2.30 (s, 3H), 6.36–6.39 (m, 2H), 6.62–6.64 (m, 2H), 6.72 (dd, 1H, J = 1.9 Hz, J = 8.8 Hz), 7.28–7.38 (m, 4H), 7.76 (d, 2H, J = 8.8 Hz), 8.76 (br s, 1H). IR: ν 1687 cm^{-1}. MS m/z: 467 $[M+23]^+$ (100).

4.1.2.20. *N*-(4-Chlorobenzyl) 1-(3,4-dichlorophenyl)-4-methyl-5-(1*H*-pyrrol-1-yl)-1*H*-pyrazole-3-carboxamide (25). Yield 62% as a white solid, mp 139 °C. ^1H NMR ($CDCl_3$): δ 2.27 (s, 3H), 4.60 (d, 2H, J = 5.9 Hz), 6.35–6.36 (m, 2H), 6.60–6.62 (m, 2H), 6.68 (dd, 1H, J = 1.7 Hz, J = 8.8 Hz), 7.22–7.33 (m, 6H), 7.37 (br t, 1H, J = 5.5 Hz). IR: ν 1673 cm^{-1}. MS m/z: 482 $[M+23]^+$ (100).

4.1.2.21. *N*-[2-(4-Chlorophenyl)ethyl] 1-(3,4-dichlorophenyl)-4-methyl-5-(1*H*-pyrrol-1-yl)-1*H*-pyrazole-3-carboxamide (26). Yield 69% as a white solid, mp 127–130 °C. ^1H NMR ($CDCl_3$): δ 2.25 (s, 3H), 2.90 (t, 2H, J = 7.0 Hz), 3.60–3.71 (m, 2H), 6.35–6.37 (m, 2H), 6.60–6.61 (m, 2H), 6.64 (dd, 1H, J = 2.1 Hz, J = 8.6 Hz), 7.09 (br t, 1H, 5.9 Hz), 7.15–7.32 (mm, 6H). IR: ν 1671 cm^{-1}. MS m/z: 474 $[M+1]^+$, 496 $[M+23]^+$, 969 $[2M+23]^+$ (100).

4.1.2.22. *N*-Cyclopentyl 1-(3,4-dichlorophenyl)-4-methyl-5-(1*H*-pyrrol-1-yl)-1*H*-pyrazole-3-carboxamide (27). Yield 98% as white needles, mp 161 °C (from diethyl ether). ^1H NMR ($CDCl_3$): δ 1.52–1.78 (mm, 6H), 2.01–2.12 (m, 2H), 2.25 (s, 3H), 4.33–4.43 (m, 1H), 6.34 (s, 2H), 6.58–6.59 (m, 2H), 6.72 (dd, 1H, J = 2.0 Hz, J = 8.7 Hz), 6.90 (br d, J = 7.4 Hz), 7.24 (s, 1H), 7.31 (d, 1H, J = 8.8 Hz). IR: ν 1664 cm^{-1}. MS m/z: 403 $[M+1]^+$, 425 $[M+23]^+$ (100), 827 $[2M+23]^+$.

4.1.2.23. *N*-Cycloheptyl 1-(3,4-dichlorophenyl)-4-methyl-5-(1*H*-pyrrol-1-yl)-1*H*-pyrazole-3-carboxamide (28). Yield 93% as a white solid, mp 173 °C (diethyl ether). ^{1}H NMR ($CDCl_3$): δ 1.52–1.67 (mm, 8H), 2.02–2.17 (m, 2H), 2.24 (s,3H), 4.05–4.19 (m, 1H), 6.34 (s, 2H), 6.58 (s, 2H), 6.72 (d, 1H, J = 10.1 Hz), 6.92 (br d, 1H, J = 8.2 Hz), 7.23 (s, 1H), 7.31 (d, 1H, J = 8.8 Hz). IR: ν 1661 cm^{-1}. MS *m/z*: 431 [M+1]$^+$, 453 [M+23]$^+$ (100), 883 [2M+23]$^+$.

4.1.2.24. *N*-(Adamant-1-yl) 1-(3,4-dichlorophenyl)-4-methyl-5-(1*H*-pyrrol-1-yl)-1*H*-pyrazole-3-carboxamide (29). Yield 97% as a white solid, mp 179–182 °C. ^{1}H NMR ($CDCl_3$): δ 1.71–1.81 (mm, 6H), 2.13–2.19 (mm, 9H), 2.23 (s, 3H), 6.33 (s, 2H), 6.58 (s, 2H), 7.72 (dd, 1H, J = 1.7 Hz, J = 7.9 Hz), 7.22 (d, 1H, J = 1.8 Hz), 7.30 (d, 1H, J = 8.5 Hz). IR: ν 1673 cm^{-1}. MS *m/z*: 470 [M+1]$^+$ (100), 961 [2M+23]$^+$.

4.1.2.25. (*R*)-*N*-[1-(1-Cyclohexyl)ethyl] 1-(3,4-dichlorophenyl)-4-methyl-5-(1*H*-pyrrol-1-yl)-1*H*-pyrazole-3-carboxamide (30). Yield 80% as a colorless oil. ^{1}H NMR ($CDCl_3$): δ 1.20 (d, 3H, J = 6.6 Hz), 1.08–1.38 (m, 4H), 1.39–1.46 (m, 1H), 1.67–1.85 (m, 6H), 2.25 (s, 3H), 3.98–4.09 (m, 1H), 6.34 (s, 2H), 6.59 (s, 2H), 6.74 (dd, 1H, J = 1.7 Hz, J = 9.9 Hz), 6.82 (d, 1H, J = 9.2 Hz), 7.31 (d, 1H, J = 8.6 Hz). IR: ν 1662 cm^{-1}. MS *m/z*: 446 [M+1]$^+$ (100), 468 [M+23]$^+$, 913 [2M+23]$^+$.

4.1.2.26. (S)-*N*-[1-(1-Cyclohexyl)ethyl] 1-(3,4-dichlorophenyl)-4-methyl-5-(1*H*-pyrrol-1-yl)-1*H*-pyrazole-3-carboxamide (31). Yield 97% as a colorless oil. ^{1}H NMR ($CDCl_3$): δ 1.19 (d, 3H, J = 6.8 Hz), 1.05–1.32 (m, 4H), 1.37–1.45 (m, 1H), 1.66–1.84 (mm, 6H),2.25 (s, 3H), 4.00–4.09 (m, 1H), 6.32–6.33 (m, 2H), 6.58–6.59 (m, 2H), 6.73 (dd, 1H, J = 2.6 Hz, J = 8.8 Hz), 6.82 (br d, 1H, J = 9.4 Hz), 7.23 (d, 1H, J = 2.7 Hz), 7.30 (d, 1H, J = 8.8 Hz). IR: ν 1651 cm^{-1}. MS *m/z*: 446 [M+1]$^+$ (100), 468 [M+23]$^+$, 913 [2M+23]$^+$.

4.1.2.27. *N*-(4-Chlorophenyl) 1-(3,4-dichlorophenyl)-5-(2,5-dimethyl-1*H*-pyrrol-1-yl)-4-methyl-1*H*-pyrazole-3-carboxamide (32). Yield 77% as a white solid, mp 190 °C. ^{1}H NMR ($CDCl_3$): δ 1.87 (s, 6H), 2.26 (s, 3H), 5.98 (s, 2H), 6.66 (dd, 1H, J = 2.8 Hz, J = 8.8 Hz), 7.26–7.37 (m, 4H), 7.68 (d, 2H, J = 8.8 Hz), 8.81 (s, 1H). IR: ν 1694 cm^{-1}. MS *m/z*: 495 [M+23]$^+$ (100), 969 [2M+23]$^+$.

4.1.2.28. *N*-(4-Chlorobenzyl) 1-(3,4-dichlorophenyl)-5-(2,5-dimethyl-1*H*-pyrrol-1-yl)-4-methyl-1*H*-pyrazole-3-carboxamide (33). Yield 97% as a white solid, mp 157 °C. ^{1}H NMR ($CDCl_3$): δ 1.85 (s, 6H), 2.23 (s, 3H), 4.61 (d, 2H, J = 6.1 Hz), 5.96 (s, 2H), 6.57 (dd, 1H, J = 2.6 Hz, J = 8.8 Hz), 7.21–7.35 (m, 6H), 7.47 (br t, 1H, J = 6.1 Hz). IR: ν 1673 cm^{-1}. MS *m/z*: 510 [M+23]$^+$ (100).

4.1.2.29. *N*-[2-(4-Chlorophenyl)ethyl] 1-(3,4-dichlorophenyl)-5-(2,5-dimethyl-1*H*-pyrrol-1-yl)-4-methyl-1*H*-pyrazole-3-carboxamide (34). Yield 90% as a pale yellow solid, mp 135 °C. ^{1}H NMR ($CDCl_3$): δ 1.84 (s, 6H), 2.21 (s, 3H), 2.93 (t, 2H, J = 7.1 Hz), 3.63–3.73 (m, 2H), 5.96 (s, 2H), 6.53 (dd, 1H, J = 2.2 Hz, J = 8.9 Hz), 7.12 (br t, 1H, J = 5.9 Hz), 7.19–7.30 (m, 6H). IR: ν 1667 cm^{-1}. MS *m/z*: 503 [M+1]$^+$ (100), 525 [M+23]$^+$.

4.1.2.30. *N*-Cyclopentyl 1-(3,4-dichlorophenyl)-5-(2,5-dimethyl-1*H*-pyrrol-1-yl)-4-methyl-1*H*-pyrazole-3-carboxamide (35). Yield 82% as a white solid, mp 168 °C. ^{1}H NMR ($CDCl_3$): δ 1.52–1.80 (mm, 6H), 1.84 (s, 6H), 2.04–2.19 (m, 2H), 2.20 (s, 3H), 4.35–4.49 (m, 1H), 5.95 (s, 2H), 6.61 (dd, 1H, J = 2.8 Hz, J = 8.8 Hz), 6.93 (br d, 1H, J = 7.4 Hz), 7.22 (d, 1H, J = 2.7 Hz), 7.31 (d, 1H, J = 8.8 Hz). IR: ν 1669 cm^{-1}. MS *m/z*: 431 [M+1]$^+$, 453 [M+23]$^+$ (100).

4.1.2.31. *N*-Cycloheptyl 1-(3,4-dichlorophenyl)-5-(2,5-dimethyl-1*H*-pyrrol-1-yl)-4-methyl-1*H*-pyrazole-3-carboxamide (36). Yield 89% as a white solid, mp 166 °C. ^{1}H NMR ($CDCl_3$): δ 1.52–1.70 (mm, 8H), 1.84 (s, 6H), 2.05–2.11 (m, 4H), 2.20 (s, 3H), 4.06–4.22 (m, 1H), 5.95 (s, 2H), 6.61 (dd, 1H, J = 2.2 Hz, J = 2.8 Hz), 6.95 (br d, 1H, J = 8.2 Hz), 7.22 (d, 1H, J = 2.1 Hz), 7.32 (d, 1H, J = 8.8 Hz). IR: ν 1667 cm^{-1}. MS *m/z*: 459 [M+1]$^+$, 481 [M+23]$^+$ (100), 939 [2M+23]$^+$.

4.1.2.32. *N*-(Adamant-1-yl) 1-(3,4-dichlorophenyl)-5-(2,5-dimethyl-1*H*-pyrrol-1-yl)-4-methyl-1*H*-pyrazole-3-carboxamide (37). Yield 90% as a white solid, mp 208–210 °C. ^{1}H NMR ($CDCl_3$): δ 1.62–1.74 (mm, 4H), 1.82 (s, 6H), 2.09–2.17 (mm, 7H), 5.92 (s, 2H), 6.60 (dd, 1H, J = 2.7 Hz, J = 8.8 Hz), 6.77 (br s, 1H), 7.19 (d, 1H, J = 2.0 Hz), 7.29 (d, 1H, J = 8.8 Hz). IR: ν 1668 cm^{-1}. MS *m/z*: 498 [M+1]$^+$, 520 [M+23]$^+$, 1017 [2M+23]$^+$ (100).

4.1.2.33. *N*-[1-(1-Phenyl)ethyl] 1-(3,4-dichlorophenyl)-5-(2,5-dimethyl-1*H*-pyrrol-1-yl)-4-methyl-1*H*-pyrazole-3-carboxamide (38). Yield 95% as a white solid, mp140–142 °C. ^{1}H NMR ($CDCl_3$): δ 1.65 (d, 3H, J = 6.9 Hz), 1.84 (s, 3H), 1.86 (s, 3H), 2.21 (s, 3H), 5.29–5.43 (m, 1H), 6.64 (dd, 1H, J = 1.9 Hz, J = 8.7 Hz), 7.21–7.37 (m, 5H), 7.40–7.47 (m, 2H). IR: ν 1663 cm^{-1}. MS *m/z*: 468 [M+1]$^+$ (100), 490 [M+23]$^+$, 957 [2M+23]$^+$.

4.1.2.34. *N*-(4-Chlorobenzhydryl) 1-(3,4-dichlorophenyl)-5-(2,5-dimethyl-1*H*-pyrrol-1-yl)-4-methyl-1*H*-pyrazole-3-carboxamide (39). Yield 98% as a white solid, mp 98–100 °C. ^{1}H NMR ($CDCl_3$): δ 1.87 (s, 6H), 2.23 (s, 3H), 5.98 (s, 2H), 6.46 /d, 1H, J = 8.2 Hz), 6.68 (dd, 1H, J = 2.3 Hz, J = 8.8 Hz), 7.20 (s, 1H), 7.28–7.42 (m, 8H), 7.63 (d, 1H, J = 8.2 Hz). IR: ν 1673 cm^{-1}. MS *m/z*: 564 [M+1]$^+$, 586 [M+23]$^+$ (100).

4.1.2.35. *N*-(4-Chlorophenyl) 1-(2,4-difluorophenyl)-4-methyl-5-(1*H*-pyrrol-1-yl)-1*H*-pyrazole-3-carboxamide (40). Yield 98% as colorless needles, mp 203 °C (from diethyl ether/*n*-hexane). ^{1}H NMR ($CDCl_3$): δ 2.32 (s, 3H), 6.22 (t, 2H, J = 2.0 Hz), 6.58 (t, 2H, J = 1.8 Hz), 6.84–6.97 (m, 2H), 7.27–7.35 (m, 3H), 7.62 (d, 2H, J = 8.8 Hz), 8.74 (br s, 1H). IR: ν 1688 cm^{-1}. MS *m/z*: 413 [M+1]$^+$, 435 [M+23]$^+$ (100).

4.1.2.36. *N*-(4-Chlorobenzyl) 1-(2,4-difluorophenyl)-4-methyl-5-(1*H*-pyrrol-1-yl)-1*H*-pyrazole-3-carboxamide (41). Yield 80% as a white solid, mp 110 °C. ^{1}H NMR ($CDCl_3$): δ 2.29 (s, 3H), 4.56 (d, 2H, J = 6.0 Hz), 6.21 (s, 2H), 6.57 (s, 2H), 6.80–6.92 (m, 3H), 7.19–7.36 (m, 4H). IR: ν 1674 cm^{-1}. MS *m/z*: 449 [M+23]$^+$ (100), 875 [2M+23]$^+$.

4.1.2.37. *N*-(2-Bromo-3,4,5-trimethoxybenzyl) 1-(2,4-difluorophenyl)-4-methyl-5-(1*H*-pyrrol-1-yl)-1*H*-pyrazole-3-carboxamide (42). Yield 95% as a white solid, mp 50–53 °C. ^{1}H NMR ($CDCl_3$): δ 2.72 (s, 3H), 3.84 (s, 6H), 3.87 (s, 3H), 4.64 (d, 2H, J = 6.1 Hz), 6.19 (t, 2H, J = 1.9 Hz), 6.54–6.55 (m, 2H), 6.81–6.94 (m, 2H), 7.19–7.31 (m, 2H), 7.38 (br t, 1H, J = 6.1 Hz). IR: ν 1671 cm^{-1}. MS *m/z*: 562 [M+1]$^+$, 584 [M+23]$^+$ (100).

4.1.2.38. *N*-[2-(4-Chlorophenyl)ethyl] 1-(2,4-difluorophenyl)-4-methyl-5-(1*H*-pyrrol-1-yl)-1*H*-pyrazole-3-carboxamide (43). Yield 87% as a colorless oil. ^{1}H NMR ($CDCl_3$): δ 2.27 (s, 3H), 2.87 (t, 2H, J = 7.3 Hz), 3.57–3.68 (m, 2H), 6.19–6.21 (m, 2H), 6.56 (s, 2H), 6.82–6.93 (m, 3H), 7.03 (br t, 1H, J = 5.8 Hz), 7.15 (d, 2H, J = 8.4 Hz), 7.25 (d, 2H, J = 8.3 Hz). IR: ν 1669 cm^{-1}. MS *m/z*: 441 [M+1]$^+$, 463 [M+23]$^+$ (100), 903 [2M+23]$^+$.

4.1.2.39. *N*-[2-(3,4-Dichlorophenyl)ethyl] 1-(2,4-difluorophenyl)-4-methyl-5-(1*H*-pyrrol-1-yl)-1*H*-pyrazole-3-carboxamide (44). Yield 94% as a pale yellow solid, mp 78 °C. ^{1}H NMR ($CDCl_3$): δ 2.27 (s, 3H), 2.87 (t, 2H, J = 7.1 Hz), 3.58–3.68 (m, 2H), 6.20 (t, 2H, J = 2.0 Hz), 6.56 (t, 2H, J = 1.8 Hz), 6.82–6.93 (m, 3H), 6.98 (br t, 1H, J = 5.8 Hz), 7.07 (dd, 1H, J = 1.8 Hz, J = 8.7 Hz), 7.18–7.37 (m, 2H). IR: ν 1672 cm^{-1}. MS *m/z*: 498 [M+23]$^+$ (100), 973 [2M+23]$^+$.

4.1.2.40. *N*-[2-(3-Chloro-4-methoxyphenyl)ethyl] 1-(2,4-difluorophenyl)-4-methyl-5-(1*H*-pyrrol-1-yl)-1*H*-pyrazole-3-carboxamide (45). Yield 81% as a colorless oil. ^{1}H NMR ($CDCl_3$): δ 2.27 (s, 3H), 2.83 (t, 2H, J = 7.2 Hz), 3.56–3.66 (m, 2H), 3.86 (s, 3H), 6.20–6.21 (m, 2H), 6.56–6.57 (m, 2H), 6.81–6.96 (m, 3H), 6.99 (br t, 1H, J = 5.7 Hz), 7.09 (dd, 1H, J = 1.9 Hz, J = 8.0 Hz), 7.16–7.28 (m, 2H). IR: ν 1672 cm^{-1}. MS *m/z*: 471 [M+1]$^+$, 493 [M+23]$^+$ (100).

4.1.2.41. *N*-[2-(2,4-Dichlorophenyl)ethyl] 1-(2,4-difluorophenyl)-4-methyl-5-(1*H*-pyrrol-1-yl)-1*H*-pyrazole-3-carboxamide (46). Yield 83% as a white solid, mp 111 °C. ^{1}H NMR ($CDCl_3$): δ 2.27 (s, 3H), 3.02 (t, 2H, J = 7.2 Hz), 3.60–3.70 (m, 2H), 6.20–6.21 (m, 2H), 6.55–6.56 (m, 2H), 6.83–6.92 (m, 3H), 7.02 (br t, 1H, J = 6.3 Hz), 7.14–7.29 (m, 2H), 7.36 (s, 1H). IR: ν 1666 cm^{-1}. MS *m/z*: 476 [M+1]$^+$, 498 [M+23]$^+$ (100).

4.1.2.42. *N*-Cyclopentyl 1-(2,4-difluorophenyl)-4-methyl-5-(1*H*-pyrrol-1-yl)-1*H*-pyrazole-3-carboxamide (47). Yield 85% as white needles, mp 109 °C (from diethyl ether/*n*-hexane). ^{1}H NMR ($CDCl_3$): δ 1.44–1.74 (mm, 6H), 1.97–2.21 (m, 2H), 2.26 (s, 3H), 4.31–4.41 (m, 1H), 6.18 (t, 2H, J = 1.8 Hz), 6.54 (t, 2H, J = 1.8 Hz), 6.79–6.92 (m, 2H), 7.21–7.32 (m, 1H). IR: ν 1668 cm^{-1}. MS *m/z*: 371 [M+1]$^+$, 393 [M+23]$^+$ (100), 763 [2M+23]$^+$.

4.1.2.43. *N*-Cycloheptyl 1-(2,4-difluorophenyl)-4-methyl-5-(1*H*-pyrrol-1-yl)-1*H*-pyrazole-3-carboxamide (48). Yield 73% as a white solid, mp 142 °C (from diethyl ether/*n*-hexane). ^{1}H NMR ($CDCl_3$): δ 1.26–1.66 (mm, 8H), 1.97–2.07 (m, 4H), 2.26 (s, 3H), 4.06–4.14 (m, 1H), 6.19–6.20 (m, 2H), 6.54–6.56 (m, 2H), 6.82–6.92 (m, 2H), 7.22–7.33 (m, 1H). IR: ν 1668 cm^{-1}. MS *m/z*: 399 [M+1]$^+$, 421 [M+23]$^+$ (100), 819 [2M+23]$^+$.

4.1.2.44. *N*-(4-Chlorophenyl) 1-(2,4-difluorophenyl)-5-(2,5-dimethyl-1*H*-pyrrol-1-yl)-4-methyl-1*H*-pyrazole-3-carboxamide (49). Yield 80% as a pasty yellow material. ^{1}H NMR ($CDCl_3$): δ 1.91 (s, 6H), 2.22 (s, 3H), 5.81 (s, 2H), 6.86–6.96 (m, 2H), 7.10–7.21 (m, 1H), 7.29 (d, 2H, J = 8.7 Hz), 7.64 (d, 2H, J = 8.7 Hz), 8.81 (br s, 1H). IR: ν 1687 cm^{-1}. MS *m/z*: 463 [M+23]$^+$ (100).

4.1.2.45. *N*-(4-Chlorobenzyl) 1-(2,4-difluorophenyl)-5-(2,5-dimethyl-1*H*-pyrrol-1-yl)-4-methyl-1*H*-pyrazole-3-carboxamide (50). Yield 80% as a white solid, mp 148 °C. ^{1}H NMR ($CDCl_3$): δ 1.89 (s, 6H), 2.19 (s, 3H), 4.57 (d, 2H, J = 6.1 Hz), 5,79 (s, 2H), 6.81–6.92 (m, 3H), 7.05–7.17 (m, 2H), 7.29–7.34 (m, 2H). IR: ν 1673 cm^{-1}. MS *m/z*: 455 [M+1]$^+$, 477 [M+23]$^+$ (100).

4.1.2.46. *N*-(2-Bromo-3,4,5-trimethoxybenzyl) 1-(2,4-difluorophenyl)-5-(2,5-dimethyl-1*H*-pyrrol-1-yl)-4-methyl-1*H*-pyrazole-3-carboxamide (51). Yield 92% as a pale yellow oil. ^{1}H NMR ($CDCl_3$): δ 1.87 (s, 6H), 2.16 (s, 3H), 3.84 (s, 6H), 3.87 (s, 3H), 4.65 (d, 2H, J = 6.3 Hz), 5.77 (s, 2H), 6.76–6.89 (m, 3H), 7.04–7.16 (m, 1H), 7.43 (br t, 1H, J = 6.1 Hz). IR: ν 1670 cm^{-1}. MS *m/z*: 590 [M+1]$^+$, 612 [M+23]$^+$, 1201 [2M+23]$^+$ (100).

4.1.2.47. *N*-[2-(4-Chlorophenyl)ethyl] 1-(2,4-difluorophenyl)-5-(2,5-dimethyl-1*H*-pyrrol-1-yl)-4-methyl-1*H*-pyrazole-3-carboxamide (52). Yield 97% as a yellow oil. ^{1}H NMR ($CDCl_3$): δ 1.88 (s, 6H), 2.17 (s, 3H), 2.89 (t, 2H,J = 7.3 Hz), 3.59–3.69 (m, 2H), 5.79 (s, 2H), 6.82–6.93 (m, 2H), 7.03–7.10 (m, 1H), 7.16 (d, 2H, J = 8.4 Hz), 7.25 (d, 2H, J = 8.5 Hz). IR: ν 1666 cm^{-1}. MS *m/z*: 469 [M+1]$^+$, 491 [M+23]$^+$ (100).

4.1.2.48. *N*-[2-(3,4-Dichlorophenyl)ethyl] 1-(2,4-difluorophenyl)-5-(2,5-dimethyl-1*H*-pyrrol-1-yl)-4-methyl-1*H*-pyrazole-3-carboxamide (53). Yield 91% as a pale yellow solid, mp 85–87 °C. ^{1}H NMR ($CDCl_3$): δ 1.89 (s, 6H), 2.16 (s, 3H), 2.89 (t, 2H, J = 7.1 Hz), 3.59–3.69 (m, 2H), 5.79 (s, 2H), 6.82–6.94 (m, 2H), 7.02–7.15 (m, 2H), 7.31–7.38 (m, 2H). IR: ν 1671 cm^{-1}. MS *m/z*: 526 [M+23]$^+$ (100), 542 [M+39]$^+$.

4.1.2.49. *N*-[2-(3-Chloro-4-methoxyphenyl)ethyl] 1-(2,4-difluorophenyl)-5-(2,5-dimethyl-1*H*-pyrrol-1-yl)-4-methyl-1*H*-pyrazole-3-carboxamide (54). Yield 80% as a yellow oil. ^{1}H NMR ($CDCl_3$): δ 1.88 (s, 6H), 2.16 (s, 3H), 2.84 (t, 2H, J = 7.3 Hz), 3.57–3.68 (m, 2H), 3.86 (s, 3H), 5.79 (s, 2H), 6.82–6.91 (m, 3H), 7.08–7.16 (m, 2H), 7.25 (d, 1H, J = 2.0 Hz). IR: ν 1666 cm^{-1}. MS *m/z*: 499 [M+1]$^+$, 521 [M+23]$^+$ (100).

4.1.2.50. *N*-[2-(2,4-Dichlorophenyl)ethyl] 1-(2,4-difluorophenyl)-5-(2,5-dimethyl-1*H*-pyrrol-1-yl)-4-methyl-1*H*-pyrazole-3-carboxamide (55). Yield 85% as a white solid, mp 121 °C. ^{1}H NMR ($CDCl_3$): δ 1.89 (s, 6H), 2.17 (s, 3H), 3.04 (t, 2H, J = 7.3 Hz), 3.61–3.72 (m, 2H), 5.79 (s, 2H), 6.82–6.94 (m, 2H), 7.03–7.10 (m, 2H), 7.15–7.21 (m, 2H), 7.37 (d, 1H, J = 1.666 Hz). IR: ν 16 cm^{-1}. MS *m/z*: 526 [M+23]$^+$ (100).

4.1.2.51. *N*-Cyclopentyl 1-(2,4-sifluorophenyl)-5-(2,5-dimethyl-1*H*-pyrrol-1-yl)-4-methyl-1*H*-pyrazole-3-carboxamide (56). Yield 83% as a white solid, mp 121 °C.^{1}H NMR ($CDCl_3$): δ 1.46–1.84 (mm, 6H), 1.87 (s, 6H), 1.98–2.10 (m, 2H), 2.15 (s, 3H), 4.32–4.43 (m, 1H), 5.77 (s, 2H), 6.81–6.91 (m, 2H), 7.07–7.19 (m, 1H). IR: ν 1661 cm^{-1}. MS *m/z*: 399 [M+1]$^+$, 421 [M+23]$^+$ (100), 819 [2M+23]$^+$.

4.1.2.52. *N*-Cycloheptyl 1-(2,4-difluorophenyl)-5-(2,5-dimethyl-1*H*-pyrrol-1-yl)-4-methyl-1*H*-pyrazole-3-carboxamide (57). Yield 86% as a white solid, mp 126 °C. ^{1}H NMR ($CDCl_3$): δ 1.50–1.82 (mm, 8H), 1.87 (s, 6H), 1.97–2.07 (m, 4H), 2.14 (s, 3H), 4.05–4.12 (m, 1H), 5.76 (s, 2H), 6.79–6.93 (m, 2H), 7.07–7.18 (m, 1H). IR: ν 1660 cm^{-1}. MS *m/z*: 427 [M+1]$^+$, 449 [M+23]$^+$ (100), 875 [2M+23]$^+$.

4.2. Molecular modeling

4.2.1. Computational chemistry

Molecular modeling and graphics manipulations were performed using the molecular operating environment (MOE)[20] and UCSF-CHIMERA[21] software packages, running on a 2 CPU (PIV 2.0–3.0 GHZ) Linux workstation. Energy minimizations and MD simulations were performed by means of AMBER 9 software,[22] selecting the Cornell force field.[23]

4.2.2. Residue indexing

The convention used for the amino acid identifiers, according to the approach of Ballesteros and Weinstein[24] and van Rhee and Jacobson,[25] facilitates comparison of aligned residues within the family of Group A GPCRs. The most conserved residue in a given TM (TMX, where X is the TM number) is assigned the number X.50, and residues within a given TM are then indexed relative to the 50 position.

4.2.3. Docking simulations

The core structures of compounds **31** and **37** were constructed using standard bond lengths and bond angles of the MOE fragment library. Geometry optimizations were accomplished with the MMFF94X force field available inside MOE. Docking simulations were carried out starting from the previously published inactive state of hCB_1 receptor model,[7] which was built using the 2.8 Å crystal structure of bovine rhodopsin (PDB entry code 1F88)[26] as a structural template. Additional details regarding the receptor structure, site-directed mutagenesis data and methods applied in developing the hCB_1 receptor model were also reported.[7] Compounds **31** and **37** were docked into the energy-minimized receptor model by means of GOLD, 4.0 version,[18] a genetic algorithm-based software, taking the binding orientation of **1** in the hCB_1

bundle[7] as a starting point. The region of interest used by GOLD was defined in order to contain the residues within 15 Å from the original position of **1** in the hCB_1 model.[7] The 'allow early termination' option was deactivated while the remaining GOLD default parameters were used. The ligands were submitted to 100 genetic algorithm runs by selecting GOLDScore as a fitness function, without any other constraints. The best docked conformation for GOLDScore was then compared with the binding conformation of **1** in the hCB_1 bundle[7] and the root-mean-square deviation between the positions of the heavy atoms was calculated, this parameter being considered as a measure of the docking accuracy.

4.2.4. Md simulations

Refinement of the ligand/receptor complexes was achieved by in vacuo energy minimization with the SANDER module of AMBER, applying an energy penalty force constant of 10 kcal mol^{-1} $Å^{-2}$ on the protein backbone atoms. The geometry-optimized complexes were then used as the starting point for subsequent 1 ns MD simulation, during which the protein backbone atoms were constrained by means of decreasing force constants; the salt bridge between K3.28(192) and D6.58(366) as well as the H-bond between the ligand carboxamide oxygen and K3.28(192) were also restrained. More specifically, an initial restraint with a force constant of 10 kcal mol^{-1} $Å^{-2}$ was applied on all the alpha carbons; this force constant decreased during the whole MD, and in the last 200 ps, its value was 0.01 kcal mol^{-1} $Å^{-2}$. Regarding the intra-helix K3.28(192)/D6.58(366) H-bonds and the ligand/K3.28(192) interactions, restraints of 10 and 50 kcal mol^{-1} $Å^{-2}$ were applied for 600 ps of MD simulation; in the last 400 ps, the restraint was removed.

General AMBER force field (GAFF) parameters were assigned to ligands, while the partial charges were calculated using the AM1-BCC method as implemented in the ANTECHAMBER suite of AMBER. A time step of 1 fs and a non-bonded pairlist updated every 25 fs were used for the MD simulations. The temperature was regulated by the way of Langevin dynamics, with a collision frequency $\gamma = 1.0$ ps^{-1}. An average structure was calculated from the last 100 ps trajectory and energy-minimized using the steepest descent and conjugate gradient methods as specified above. Root mean square (rms) deviations from the initial structures and interatomic distances were monitored using the PTRAJ module in AMBER.

4.3. CB_1 and CB_2 receptor binding assays

For both receptor binding assays, the new compounds were tested as previously described.[8]

4.4. In vivo pharmacological studies

The experimental procedure used in the present study was in strict accordance with the Italian Law on the 'Protection of animals used for experimental and other scientific reasons'.

4.4.1. Animals

Adult male Wistar rats (Charles River Laboratories, Calco, Italy), weighing approximately 400 g at the time of the tests, were used. Rats were individually housed in standard plastic cages with wood chip bedding. The animal facility was under an inverted 12:12 h light–dark cycle (lights on at 11:00 pm), at a constant temperature of 22 ± 2 °C and relative humidity of approximately 60%. Rats were extensively habituated to handling and intraperitoneal injection. Food pellets (standard rat chow; Harlan, San Pietro al Natisone, Italy) and water were available 24 h/day.

4.4.2. Experimental procedure

Two independent experiments were conducted, one testing compound **4** and the other testing compound **52**. On the test day of each experiment, rats were divided into four groups of $n = 6–8$, matched for body weight and food intake over the 3 days preceding the start of the experiment, and treated with 0, 0.1, 1, and 10 mg/kg of compounds **4** or **52**. Compounds **4** and **52** were suspended in saline with a few drops of Tween 80 and administered intraperitoneally (injection volume: 1 mL/kg) 30 min before lights off. Food and water intake was recorded 60, 120, 180, 240, 300, 360, and 1440 min after lights off (1440 min correspond to 24 h) by weighing food pellets and bottles with a 0.1-g accuracy. Data on the effect of compounds **4** or **52** on cumulative food and water intake over the first 360 min were analyzed by separate 2-way (treatment; time) ANOVAs with repeated measures on the factor 'time', followed by the Newman-Keuls test for *post hoc* comparisons; data on the effect of compounds **4** or **52** on food and water intake at the 1440-min time interval were analyzed by separate 1-way ANOVAs.

Acknowledgements

Authors from the University of Siena wish to thank the Ministero dell'Università e della Ricerca (PRIN 2006—Prot. n 2006030948_002) for financial support.

Supplementary data

Supplementary data associated with this article can be found, in the online version, at doi:10.1016/j.bmc.2009.06.027.

References and notes

1. (a) Di Marzo, V. *Nat. Rev. Drug Discovery* **2008**, *7*, 438; (b) Lambert, D. M.; Fowler, C. J. *J. Med. Chem.* **2005**, *48*, 5059; (c) Pavlopoulos, S.; Thakur, G. A.; Nikas, S. P.; Makriyannis, A. *Curr. Pharm. Des.* **2006**, *12*, 1751; (d) Maione, S.; Starowicz, K.; Palazzo, E.; Rossi, F.; Di Marzo, V. *Drug Dev. Res.* **2006**, *67*, 339; (e) Bifulco, M.; Laezza, C.; Gazzerro, P.; Pentimalli, F. *Oncol. Rep.* **2007**, *17*, 813; (f) Hillard, C. J. *Curr. Pharm. Des.* **2008**, *14*, 2347; (g) Di Filippo, M.; Picconi, B.; Tozzi, A.; Ghiglieri, V.; Rossi, A.; Calabresi, P. *Curr. Pharm. Des.* **2008**, *14*, 2337; (h) Bellocchio, L.; Mancini, G.; Vicennati, V.; Pasquali, R.; Pagotto, U. *Curr. Opin. Pharm.* **2006**, *6*, 586; (i) Baker, D.; Pryce, G. *Curr. Pharm. Des.* **2008**, *14*, 2326–2336; (j) Pazos, M. R.; Sagredo, O.; Fernandez-Ruiz, J. *Curr. Pharm. Des.* **2008**, *14*, 2317–2325; (k) Bilsland, L. G.; Greensmith, L. *Curr. Pharm. Des.* **2008**, *14*, 2306–2316; (l) Storr, M. A.; Yuece, B.; Andrews, C. N.; Sharkey, K. A. *Neurogastroenterol. Motility* **2008**, *20*, 857; (m) Szmitko, P. E.; Verma, S. *Atherosclerosis* **2008**, *199*, 248–256; (n) Bifulco, M.; Malfitano, A. M.; Pisanti, S.; Laezza, C. *Endocr.-Relat. Cancer* **2008**, *15*, 391; (o) Mach, F.; Steffens, S. *J. Neuroendocrinol.* **2008**, *20*, S1:53; (p) Nesto, R. W.; Mackie, K. *Eur. Heart J. Supp.* **2008**, *10*, B34; (q) Bisogno, T.; Di Marzo, V. *Curr. Pharm. Des.* **2008**, *14*, 2299.
2. Sorbera, L. A.; Castaner, J.; Silvestre, J. S. *Drugs Future* **2005**, *30*, 128.
3. (a) Padwal, R. S.; Majumdar, S. R. *Lancet* **2007**, *369*, 71; (b) Doggrell, S. A. *Exp. Opin. Pharmacother.* **2008**, *9*, 2727.
4. Press release Sanofi-aventis, 2008, October 23.
5. (a) Representative examples of bioisosteric analogues of **1** are depicted in our previous paper (see Ref. 7).; (b) Representative literature for non-bioisosteric analogues of **1**: (b1) Griffith, D. A.; Hadcock, J. R.; Black, S. C.; Iredale, P. A.; Carpino, P. A.; Da Silva-Jardine, P.; Day, R.; DiBrino, J.; Dow, R. L.; Landis, M. S.; O'Connor, R. E.; Scott, D. O. *J. Med. Chem.* **2009**, *52*, 234.; (b2) Dow, R. L.; Carpino, P. A.; Hadcock, J. R.; Black, S. C.; Iredale, P. A.; DaSilva-Jardine, P.; Schneider, S. R.; Paight, E. S.; Griffith, D. A.; Scott, D. O.; O'Connor, R. E.; Nduaka, C. I. *J. Med. Chem.* **2009**, *52*, 2652; (b3) Debenham, J. S.; Madsen-Duggan, C. B.; Wang, J.; Tong, X.; Lao, J.; Fong, T. M.; Schaeffer, M.-T.; Xiao, J. C.; Huang, C. C. R.-R.; Shen, C.-P.; Stribling, D. S.; Shearman, L. P.; Strack, A. M.; MacIntyre, D. E.; Hale, J. J.; Walsh, T. F. *Bioorg. Med. Chem. Lett.* **2009**, *19*, 2591; (b4) Smith, R. A.; Fathi, Z.; Brown, S.-E.; Choi, S.; Fan, J.; Jenkins, S.; Kluender, H. C. E.; Konkar, A.; Lavoie, R.; Mays, R.; Natoli, J.; O'Connor, S. J.; Ortiz, A. A.; Podlogar, B.; Taing, C.; Tomlinson, S.; Tritto, T.; Zhang, Z. *Bioorg. Med. Chem. Lett.* **2007**, *17*, 673.
6. For example see: (a) Silvestri, R.; La Regina, G.; De Martino, G.; Artico, A.; Befani, O.; Palumbo, M.; Agostinelli, E.; Turini, P. *J. Med. Chem.* **2003**, *46*, 917; (b) Silvestri, R.; Artico, M.; La Regina, G.; De Martino, G.; La Colla, M.; Loddo, R.; La Colla, P. *Farmaco* **2004**, *59*, 201; (c) Silvestri, R.; Marfè, G.; Artico, M.; La Regina, G.; De Martino, G.; Lavecchia, A.; Novellino, E.; Morgante, E.; Di Stefano, C.; Catalano, G.; Filomeni, G.; Abruzzese, E.; Ciriolo, M. R.; Russo, M. A.; Amadori, S.; Cirilli, R.; La Torre, F.; Sinibaldi Salimei, P. *J. Med. Chem.* **2006**, *49*, 5840.
7. Silvestri, R.; Cascio, M. G.; La Regina, G.; Piscitelli, F.; Lavecchia, A.; Brizzi, A.; Pasquini, S.; Botta, M.; Novellino, E.; Di Marzo, V.; Corelli, F. *J. Med. Chem.* **2008**, *51*, 1560.
8. Brizzi, A.; Brizzi, V.; Cascio, M. G.; Bisogno, T.; Siriani, R.; Di Marzo, V. *J. Med. Chem.* **2005**, *48*, 7343.

9. Cheng, Y.; Prusoff, W. H. *Biochem. Pharmacol.* **1973**, *22*, 3099–3108.
10. Colombo, G.; Agabio, R.; Diaz, G.; Lobina, C.; Reali, R.; Gessa, G. L. *Life Sci.* **1998**, *63*, PL113.
11. DiMarzo, V.; Goparaju, S. K.; Wang, L.; Liu, J.; Bátkai, S.; Járai, Z.; Fezza, F.; Miura, G. I.; Palmiter, R. D.; Sugiura, T.; Kunos, G. *Nature* **2001**, *410*, 822.
12. Kapur, A.; Hurst, D. P.; Fleischer, D.; Whitnell, R.; Thakur, G. A.; Makriyannis, A.; Reggio, P. H.; Abood, M. E. *Mol. Pharmacol.* **2007**, *71*, 1512.
13. Hurst, D.; Umejiego, U.; Lynch, D.; Seltzman, H.; Hyatt, S.; Roche, M.; McAllister, S.; Fleischer, D.; Kapur, A.; Abood, M.; Shi, S.; Jones, J.; Lewis, D.; Reggio, P. *J. Med. Chem.* **2006**, *49*, 5969.
14. McAllister, S. D.; Rizvi, G.; Anavi-Goffer, S.; Hurst, D. P.; Barnett-Norris, J.; Lynch, D. L.; Reggio, P. H.; Abood, M. E. *J. Med. Chem.* **2003**, *46*, 5139.
15. Hurst, D. P.; Lynch, D. L.; Barnett-Norris, J.; Hyatt, S. M.; Seltzman, H. H.; Zhong, M.; Song, Z. H.; Nie, J.; Lewis, D.; Reggio, P. H. *Mol. Pharmacol.* **2002**, *62*, 1274.
16. Salo, O. M. H.; Lahtela-Kakkonen, M.; Gynther, J.; Jarvinen, T.; Poso, A. *J. Med. Chem.* **2004**, *47*, 3048.
17. Shen, C.-P.; Xiao, J. C.; Armstrong, H.; Hagmann, W. K.; Fong, T. M. *Eur. J. Pharmacol.* **2006**, *15*, 41.
18. (a) GOLD, version 4.0; CCDC Software Limited: Cambridge, UK, 2008.; (b) Jones, G.; Willett, P.; Glen, R. C.; Leach, A. R.; Taylor, R. *J. Mol. Biol.* **1997**, *267*, 727.
19. Lin, L. S.; Ha, S.; Ball, R. G.; Tsou, N. N.; Castonguay, L. A.; Doss, G. A.; Fong, T. M.; Shen, C. P.; Xiao, J. C.; Goulet, M. T.; Hagmann, W. K. *J. Med. Chem.* **2008**, *51*, 2108.
20. Molecular Operating Environment (MOE), version 2005.06; Chemical Computing Group, Inc.: Montreal, Canada, 2005.
21. Huang, C. C.; Couch, G. S.; Pettersen, E. F.; Ferrin, T. E. *Pac. Symp. Biocomput.* **1996**, *1*, 724. http://www.cgl.ucsf.edu/chimera.
22. Case, D. A.; Darden, T. A.; Cheatham, T. E., III; Simmerling, C. L.; Wang, J.; Duke, R. E.; Luo, R.; Merz, K. M.; Pearlman, D.A.; Crowley, M.; Walker, R.C.; Zhang, W.; Wang, B.; Hayik, S.; Roitberg, A.; Seabra, G.; Wong, K.F.; Paesani, F.; Wu, X.; Brozell, S.; Tsui, V.; Gohlke, H.; Yang, L.; Tan, C.; Mongan, J.; Hornak, V.; Cui, G.; Beroza, P.; Mathews, D.H.; Schafmeister, C.; Ross, W.S.; Kollman, P.A. AMBER 9; University of California, San Francisco, 2006.
23. Cornell, W. D.; Cieplak, P.; Bayly, C. I.; Gould, I. R.; Merz, K. M., Jr.; Ferguson, D. M.; Spellmeyer, D. C.; Fox, T.; Caldwell, J. W.; Kollman, P. A. *J. Am. Chem. Soc.* **1995**, *117*, 5179.
24. Ballesteros, J. A.; Weinstein, H. *Methods Neurosci.* **1995**, *25*, 366.
25. van Rhee, A. M.; Jacobson, K. A. *Drug Dev. Res.* **1996**, *37*, 1.
26. Palczewski, K.; Kumasaka, T.; Hori, T.; Behnke, C. A.; Motoshima, H.; Fox, B. A.; Trong, I. L.; Teller, D. C.; Okada, T.; Stenkamp, R. E.; Yamamoto, M.; Miyano, M. *Science* **2000**, *289*, 739.